Microchimica Acta (2020) 187: 549
https://doi.org/10.1007/s00604-020-04526-x

REVIEW ARTICLE

Recent advances in aptamer-based sensors for breast cancer diagnosis: special cases for nanomaterial-based VEGF, HER2, and MUC1 aptasensors

Samet Şahin[1] · Mustafa Oguzhan Caglayan[1] · Zafer Üstündağ[2]

Received: 21 May 2020 / Accepted: 20 August 2020 / Published online: 4 September 2020

Abstract

Cancer is one of the most common and important diseases with a high mortality rate. Breast cancer is among the three most common types of cancer in women, and the mortality rate has reached 0.024% in some countries. For early-stage preclinical diagnosis of breast cancer, sensitive and reliable tools are needed. Today, there are many types of biomarkers that have been identified for cancer diagnosis. A wide variety of detection strategies have also been developed for the detection of these biomarkers from serum or other body fluids at physiological concentrations. Aptamers are single-stranded DNA or RNA oligonucleotides and promising in the production of more sensitive and reliable biosensor platforms in combination with a wide range of nanomaterials. Conformational changes triggered by the target analyte have been successfully applied in fluorometric, colorimetric, plasmonic, and electrochemical-based detection strategies. This review article presents aptasensor approaches used in the detection of vascular endothelial growth factor (VEGF), human epidermal growth factor receptor 2 (HER2), and mucin-1 glycoprotein (MUC1) biomarkers, which are frequently studied in the diagnosis of breast cancer. The focus of this review article is on developments of the last decade for detecting these biomarkers using various sensitivity enhancement techniques and nanomaterials.

Keywords Breast cancer · Aptasensor · Biosensor · Cancer biomarker · VEGF · MUC1 · HER2

Introduction

According to the National Cancer Institute's report, 1,735,350 new cancer cases were diagnosed in the USA and there were 609,640 deaths due to cancer in 2018. It is estimated that cancer cases and the number of cancer-related deaths are going to be 1,762,450 and 606,880 in 2019, respectively (2020 data has not yet been announced) [1]. The most common types of cancer can be listed as lung, chest, prostate, colon, rectum, skin melanoma, Hodgkin lymphoma, thyroid, liver, renal pelvis, endometrial, leukemia, and pancreatic cancer [2]. The 3 most common cancer deaths among women were lung, breast, and colorectal in which 231,840 women were diagnosed and 40,290 died in 2015 with breast cancer in the USA [3]. Each year, globally approximately 521,900 deaths have been reported due to invasive breast cancer, the second leading cause of cancer death [4, 5]. Breast cancer morbidity is high due to distant metastases and has reached 0.024% in some countries [6, 7].

Early diagnosis is vital to improve the survival rate by reducing cancer incidence rates and mortality in breast cancer, similar to all types of cancer. Traditional breast cancer diagnostic tools include various complex techniques such as clinical and physical examinations, histopathology, imaging mammography, ultrasound, magnetic resonance imaging, X-ray, computed tomography, positron emission tomography, cytology, and biopsy [8]. Existing technologies and methods are often successful; however, some of these techniques are invasive, expensive, time-consuming, give false-positive results, or subject to radiation, which is an additional risk factor. Moreover, laboratories with sophisticated infrastructure are needed for their implementation. Besides, molecular tools such as quantitative polymerase chain reaction, enzyme-

✉ Samet Şahin
samet.sahin@bilecik.edu.tr

✉ Mustafa Oguzhan Caglayan
oguzhan.caglayan@gmail.com

[1] Department of Bioengineering, Bilecik Şeyh Edebali University, 11230 Bilecik, Turkey

[2] Department of Chemistry, Kütahya Dumlupınar University, 43100 Kütahya, Turkey

linked immunosorbent assay (ELISA), radioimmunoassay, immunohistochemistry, and flow cytometry are also used in the diagnosis of breast cancer [9, 10]. However, most of these approaches are also expensive, require highly qualified personnel, time-consuming, and laboratory-dependent. Therefore, non-invasive, simple, and low-risk methods are needed for screening or diagnosing breast cancer at the point of care (PoC) [11].

When a specific biological molecule that is a sign of cancer is found in body fluids (such as blood), or tissues, early and minimally invasive detection of cancer using those biomarkers can be performed [12]. Rapid and accurate detection of cancer-specific biomarkers in various samples such as peripheral blood and serum has gained importance in the early diagnosis of breast cancer [13–15]. Circulating biomarkers for breast cancer include DNA, mRNAs, cell surface receptors, transcription factors, mucin, isoenzymes, oncogenes, oncofetal antigens, tissue-specific proteins, circulating ribonucleic acids, and several intracellular and intercellular compounds, such as glycoproteins and glycolipids [16].

Vascular endothelial growth factor (VEGF) is an important regulator of physiological vascular development during vasculogenesis in tissues [17, 18]. In mammals, VEGF has four different isoforms [19] and one of which is VEGF165, which is a biomarker associated with the development and metastasis of various cancers [20, 21]. Overexpression of VEGF is considered a possible indicator of cancers, especially to create independent blood sources due to the need for oxygen and nutrients to initiate the metastasis process [22–24]. However, although VGF is an important biomarker in breast cancer, it is also used as a serum biomarker for other cancer types [25, 26], neurological disorders, proliferative retinopathy [27], rheumatoid arthritis [28], psoriasis [29], and Parkinson's disease [30–32]. While the serum VEGF concentration in healthy subjects is 1–177 pg/mL, it can increase to 18–328 pg/mL in breast cancer patients [26, 33].

Human epidermal growth factor receptor 2 (HER2, also known as ErbB2) acts in the signaling cascade that affects cell proliferation and differentiation [34, 35]. HER2 protein overexpression is observed in 15–20% of all breast cancers [36–39] and it is associated with the most aggressive patient prognosis with a low survival rate [40, 41]. It has been reported that HER2 concentration in the blood is between 2 and 15 ng/mL in healthy individuals and 15–75 ng/mL in HER2 positive breast cancer patients [42]. Also, it has been noted that HER2 overexpression is associated with resistance to certain chemotherapeutics, risk of brain metastasis, and higher recurrence of the disease in breast cancer [43–45]. HER2 overexpression has also been reported in other types of cancer, such as stomach, ovarian, and lung cancer [46].

Furthermore, there is another biomarker that can be related to breast cancer. The mucin family is a high molecular weight glycosylated protein produced by epithelial tissues, found in most gel-like secretions, offering functions such as lubrication, cell signaling, and creating chemical barriers [47]. It has been reported that mucin-1 (MUC1) glycoprotein from this family is abnormally overexpressed in 96.7% of lung cancers, 90% of pancreatic, prostate, and epithelial ovarian cancers, and 70% of breast cancer [48–50]. The type of MUC1 expressed by cancer cells is structurally different from normal MUC1 and is, therefore, a biomarker used for the diagnosis of breast cancer in the early stages [51–54]. While healthy individuals generally have < 31 U/mL MUC1 in serum, this concentration increases 100 times in breast cancer [55, 56].

Although VEGF, HER2, and MUC1 are the most studied and well-known biomarkers for breast cancer, there are various other markers for breast cancer reported in the literature [57, 58]. Since reviewing all biomarker studies in the relevant literature is a great challenge, the context of this review is limited to VEGF, HER2, and MUC1 biomarkers. Up to this day, techniques such as ELISA [59], immunohistochemistry [30], fluorescent in situ hybridization [60], and radioimmunoassay [61] are used as the gold standard for biomarker detection to analyze VEGF, HER2, and MUC1 biomarkers [62]. Although these techniques provide sufficient analytical performance, they are often complex, expensive, labor-intensive, and time-consuming, and require complex protocols and sophisticated instruments to perform for clinical diagnoses [63–65]. Moreover, current diagnostic technologies have some limitations and the risk of false-positive results is between 20 and 50% [66]. Therefore, it is necessary to develop cost-effective sensors for the sensitive and specific detection of these biomarkers from body fluids such as blood or serum [21].

In this context, biosensors can overcome some of the limitations mentioned above due to their advantages such as high analytical specificity, cost-effectiveness, and high sensitivity [31, 32, 67]. A biosensor consists of the molecular sensing element, a transducer that converts the obtained signal into a measurable physical signal, and the analytical device from which the data is obtained. There are various transducing methods which can be utilized in biosensor design such as electrochemical, optical, electronic, piezoelectric, and gravimetric [68]. Biological elements such as enzymes, antibodies, antigens, receptors, nucleic acids, whole cells, and tissues are used in a biosensor as the sensing or recognition element, which is the most important part that affects the selectivity of a sensor [69, 70]. Recently, biosensor technology has found wide coverage in health, biomedicine, and biopharmaceutical studies [71, 72].

Several innovative approaches are used to increase the analytical performance of biosensors such as the use of the molecular diagnostic element with different utilization strategies and the incorporation of nanomaterials into the sensor platform [73–75]. In particular, the combination of nanobiosensor platforms with molecular sensing elements such as

different antibodies, peptide sequences, polymers, and aptamers are frequently preferred [71, 76].

Aptamers, a unique molecular diagnostic element, are single-stranded DNA (ssDNA), RNA, or modified nucleic acids, isolated by an in vitro selection process known as SELEX (systematic evolution of ligands with exponential enrichment) [77–81]. Aptamers have high specificity and binding affinities, similar to antibodies, because they fold into unique three-dimensional structures, by creating various secondary structures such as stem, loop, hairpin, pseudoknot, and G-quadruplex [82, 83]. Besides, they also have advantages such as rapid in vitro selection, cell-free chemical synthesis, smaller size and low complexity, resistance to denaturation and high stability, and easy chemical modification [84–86]. The interaction of aptamers and aptamer-nanomaterial conjugates with different analytes, for example, aptamer-protein complexes, allowed the development of new test strategies [30, 87]. Since their development, aptamers have been selected and reported for various targets such as metal ions [88, 89], small molecules [90], proteins [91], viruses [92], bacteria [93], and whole cells [94, 95]. An alternative to antibodies, aptamers are also an important molecular diagnostic element in breast cancer diagnosis [21, 77, 96–98].

There are several review articles in the literature summarizing valuable information on the use of aptamers in cancer diagnosis. For example, review articles provide a brief classification and description of the research progress of aptamer-based biosensors and nano-biosensors for the detection and quantitative determination of MUC1 and VEGF based on optical and electrochemical platforms [99, 100]. Other review articles also investigate aptamer selection and applications for breast cancer and the use of aptamers in colorectal cancer types in diagnosis and treatment [35, 101]. Mittal et al. reported a review article that discusses the use of glycoproteins, DNA biomarkers, micro-RNA, circulatory tumor cells, and some potential biomarkers for electrochemical sensors developed for breast cancer diagnosis [10]. Reviews of current advances in cancer measurement and analysis using electrochemical biosensors, nanomaterial-based aptasensors, and their applications in the field of clinical and environmental diagnosis, and the application of electrochemical aptasensors for clinical diagnostics, and food and environmental monitoring are also available in the literature [102–106]. However, there is no review available investigating the most used biomarkers together listing the aptamers sequences used and comparing analytical parameters per each method employed.

Herein, a special focus on aptasensors developed for the most potential biomarkers, VEGF, HER2, and MUC1, is presented. An extensive analysis of analytical performance parameters was performed for the aptasensors based on nanomaterial conjugated aptamer-based strategies. In terms of detection strategies, fluorescence and chemiluminescence-based [107, 108], colorimetric-based [109], plasmonic-based [85, 87] electrochemical-based [110, 111] approaches and other methods [112, 113] were summarized. The aptamers used in breast cancer diagnosis targeting certain biomarkers are listed in Table 1. It can be seen that DNA and RNA aptamers consisting of 17–86 bases generally have an affinity with a k_d (dissociation constant) value at nM level. Besides, more aptamers have been selected and developed for species that are also a biomarker in other types of cancer, such as VEGF. The sequences of the aptamers are also given in Table 1 in the direction of 5′-3′.

In this review, reported molar concentrations for VEGF and HER2 were calculated using molecular weights of 145,500 g/mol for HER2 and 27,000 g/mol for VEGF to obtain comparable analytical performance values. However, since MUC1 has an apparent molecular mass of 300–600 kDa, MUC1 concentrations are reported as is.

Fluorescence and chemiluminescence-based detection strategies

Fluorescence-based strategies (Table 2) are often preferred in aptasensors for the determination of biomarkers in breast cancer diagnosis due to their advantages such as high sensitivity, repeatability, and rapid detection [74, 147]. Low energy radiation emission after high energy radiation is absorbed by a dye or fluorescent nanomaterial is called fluorescent, and detection is performed by fluorescent quenching or fluorophore signal recovery strategies. In the design of fluorescent aptasensors, hairpin aptamer (aptabeacon) labeled with a fluorophore and a quencher is used.

Forster resonance energy transfer (FRET) is a method using two fluorophores as donor and acceptor, and different FRET configurations can be created by changing the types of fluorophores, quencher type, and aptamer beacons [148, 149]. Luminescence is called chemiluminescence (CL) when triggered by chemical reaction and electrochemiluminescence (ECL) when triggered by electrochemical reactions [150]. Different strategies are often applied to FRET operations that can be "signal-on" and "signal-off" depending on the binding of the aptamer to its target molecule [151].

Since the configurations of the aptamers have changed in their interactions with their targets, the switched probe technique works successfully in FRET aptasensors. This aptamer-specific approach has been successfully used in MUC1-triggered autonomic amplification by combining the G-quadruplex aptamer and PCR techniques [140]. In this approach, ssDNA synthesis and amplification were carried out with the help of DNA polymerase, and the change in the conformation of the aptamer region in the hairpin probes with MUC1 binding that releases primary complementary sequences. In this study, MUC1 was detected in the range of 5–1000 pM with a 1.9 pM limit of detection (LOD) value

Table 1 Aptamers used for the diagnosis of breast cancer

Sequence (5′-3′)	Target	Reported k_d	Ref.
CACT ACAG AGGT TGCG TCTG TCCC ACGT TGTC ATGG GGGG TTGG CCTG	Epithelial cell adhesion molecule	38 nM	[114]
GGGG UCAA GGUG ACCC C	Estrogen receptor (Erα)	1×10^8 /M (k_a)	[115]
GGGC CGTC GAAC ACGA GCAT GGTG CGTG GACC TAGG ATGA CCTG AGTA CTGT CC	HER2	270 nM	[116]
AACC GCCC AAAT CCCT AAGA GTCT GCAC TTGT CATT TTGT ATAT GTAT TTGG TTTT TGGC TCTC ACAG ACAC ACTA CACA CGCA CA	HER2	18.9 nM	[117]
CTTC TGCC CGCC TCCT TCCT GGGG CCTG GATA CGGA TTGG TAAG GATT AGTA GGGG GCAT AGCT GGAG ACGA GATA GGCG GACA CT	HER2	3.5 nM	[118]
CCGC AACC ACGA CCGA AAGA CAAC GCAA TCTG ACAC GTGG	HER2	6.33 nM	[119]
GCAG TTGA TCCT TTGG ATAC CCTG G	MUC1	1.62 μM	[120]
ACAC GGCA GTTG ATCC TTTG GATA CCCT GGCG TGT	MUC1	NR*	[53]
GCAG TTGA TCCT TTGG ATAC CCTG G	MUC1	0.135 nM	[121]
GGGA GACA AGAA TAAA CGCT CAAG CAGT TGAT CCTT TGGA TACC CTGG TTCG ACAG GAGG CTCA CAAC AGGC	MUC1	47.3 nM	[122]
TGTG GGGG TGGA CGGG CCGG GTAG A	VEGF	0.47 nM	[123]
CCGT CTTC CAGA CAAG AGTG CAGG G	VEGF	404 nM	[124]
AUGC AGUU UGAG AAGU CGCG CAU	VEGF	NR	[125]
TTTT CCCG TCTT CCAG ACAA GAGT GCAG GG	VEGF	0.9 nM	[126]
ATAC CAGT CTAT TCAA TTGC ACTC TGTG GGGG TGGA CGGG CCGG GTAG A	VEGF	20 nM	[127]
ATAC CAGT CTAT TCAA TTGG GCCC GTCC GTAT GGTG GGTG TGCT GGCC AGAT AGTA TGTG CAAT CA	VEGF	130 nM	[127]
TGTG GGGG TGGA CTGG GTGG GTAC C	VEGF	0.30 nM	[128]
CCGT CTTC CAGA CAAG AGTG CAGG G	VEGF	1.4 nM	[129]
CAAT TGGG CCCG TCCG TATG GTGG GT	VEGF	0.5 nM	[130]
ATAC CAGT CTAT TCAA TTGG GCCC GTCC GTAT GGTG GGTG TGCT GGCC AGAT AGTA TGTG CAAT CA	VEGF	120 nM	[131]

* *NR* not reported.

using a signal-on strategy with thioflavin T fluorophore. Such triggered amplification techniques have been frequently used in breast cancer biomarkers. For instance, an immunoassay coupled with an isothermal exponential amplification reaction was proposed for the MUC1, using a sandwich approach. Sandwich-type combinations were specifically formed in the immuno-PCR plate with target triggering. Then, with the help of an additional amplification template, polymerase and nicking enzyme fluorescence of SYBR Green I was amplified for detection of MUC1 with 1.63 pM LOD value [139].

A similar strategy was used for VEGF determination in cyclic signal amplification triggered in the presence of target molecules using T7 exonuclease (Exo). The ECL was induced by a G-quadruplex/hemin-DNAzyme formation to produce a "signal-off" VEGF sensor by triggering the amplification of the trigger-released aptamer with the T7 Exo. In this study, VEGF determination was performed successfully with 0.2 pM LOD value for 1 pM–20 nM detection range [144]. In the same study, not only the target-triggered amplification strategy was used, but also CdS: Eu nanoclusters (NCs) were also utilized as the ECL substrate.

Nanomaterials are frequently used in fluorescent-based detection strategies [133]. For example, using colloidal gold nanoparticles (AuNPs) or quantum dots (QDs) [149], dendrimers [152] and graphene oxide [153] have been previously reported instead of traditional organic fluorophores. QDs are semiconductor fluorescent materials, which have advantages such as size-controlled fluorescence, and higher fluorescent quantum yields, and production and modification versatility [154, 155]. However, they have some disadvantages such as toxicity, chemical instability, and low-fluorescence emission [156]. In a study using a probe consisting of a quencher, QD-labeled reporter, and the MUC1 aptamer stem, a FRET sensor was developed using the quencher and fluorescence reporter brought into proximity in the presence of MUC1. This study was one of the first studies for MUC1 determination using the structural switching feature of the aptamer and MUC1 was determined with 250 nM LOD with the "signal-off" strategy [120]. A quenching resonance energy transfer (QRET) assay using time-resolved luminescence has been reported using luminescent lanthanide-chelate labeled VEGF aptamers and VEGF

Table 2 Fluorescence and chemiluminescence-based strategies for VEGF, HER2, and MUC1 aptasensors

Method	Biomarker	Strategy	LOD	Range	Ref.
Fluorescence (signal-on)	HER2	Dual aptamer approach, separation of aptamer-conjugated AgNCs from anti-HER2 aptamer upon analyte detection, guanine-rich aptamer-conjugated AgNCs as fluorescence probe, aptabeacon format, FRET	90 aM	8.5–225 fM	[132]
Fluorescence (signal-off)	HER2	Fluorescently labeled aptamer, CNTs coupled with MBs, MB–CNT–aptamer hybrids, FRET	38 nM	50–250 nM	[116]
Fluorescence (signal-off)	HER2	GO quencher, dye-labeled MUC1 specific aptamer, FRET	0.96 nM	1.2–240 nM	[133]
Fluorescence (signal-off)	MUC1	Quencher, QD-labeled reporter, and the MUC1 aptamer stem-based 3-component DNA hybridization system, QD-labeling, aptabeacon format, FRET.	250 nM	250 nM-2 μM	[120]
Fluorescence (signal-off)	MUC1	GO quencher, dye-labeled MUC1 specific aptamer, FRET	28 nM	0.04–10 μM	[134]
Fluorescence (signal-off)	MUC1	Carbon NDs (strong blue-green fluorescence) and GO quencher FRET	17.1 nM	20.0–804.0 nM	[135]
Fluorescence sandwich (signal-off)	MUC1	Carbon NDs (strong blue-green fluorescence) and GO quencher FRET, sandwich format, antibodies (Abs) against MUC1, and the MUC1 aptamer-conjugated NDs. Aggregation of NDs due to the sandwich formation, quenching of fluorescence	2 nM	5–100 nM	[136]
Fluorescence (signal-on)	MUC1	Oxidized mesoporous carbon nanospheres conjugated with cyanine (Cy3)-labeled aptamer probe, FRET	6.52 nM	0.01–10.6 μM	[137]
Fluorescence (signal-on)	MUC1	Cyanine (Cy5)-tagged aptamer, fluorescent SiNDs, aptabeacon format, signal-on in the presence of MUC1 due to structure switching of aptamer, FRET	1.52 nM	3.33–250 nM	[138]
Fluorescence Enzymatic Amplification Sandwich (signal-on)	MUC1	Sandwich immunoassay coupled with isothermal exponential amplification reaction, PCR using amplification template, polymerase, and nicking enzyme, MUC1-triggered enzymatic amplification, SYBR Green I.	1.63 pM	3 pM–3 nM	[139]
Fluorescence Enzymatic Amplification Sandwich (signal-on)	MUC1	MUC1 triggered the autonomous synthesis of G-quadruplex sequences via primer exchange signal amplification strategy. Target molecules bind and cause the change in conformation of the aptamer region in the hairpin probes to expose the primer complementary sequences, polymerase enzyme, enzymatic amplification, G-quadruplex, thioflavin T.	1.9 pM	5 pM–1 nM	[140]
Fluorescence (signal-on)	MUC1	Polydiacetylene (PDA) liposome-based system, Cy3-labeled aptamer, structure-switching aptabeacon format, quenching via PDA, FRET.	0.8 nM	0–200 nM	[141]
Fluorescence Enzymatic Amplification (signal-on)	MUC1	Aptamer-based immuno-loop-mediated isothermal amplification, peptide, MBs, PCR	1 aM	1 aM–1 pM	[121]
Electrochemiluminescence Catalytic (signal-on)	MUC1	ECL biosensing platform, dual catalytic hairpin assembly, CdS: Mn quantum dots	0.40 fg/mL	1 fg/mL–1 ng/mL	[142]
Fluorescence (signal-on)	VEGF	Time-resolved luminescence, lanthanide(III)-chelate labeled DNA aptamers, binding of the target molecule to Ln(III)-chelate interferes with the quencher leading to the increased distance between the quencher and Ln (III) chelate, QRET assay.	NR*	0.25–10 nM	[96]
Chemiluminescence Sandwich (signal-on)	VEGF	Single-photon avalanche diode, SiO_2 substrate, horseradish peroxidase (HRP)-induced chemiluminescence, sandwich structure.	2.15 pM	NR	[86]
Chemiluminescence (signal-on)	VEGF	Aptamer controlled catalysis, positively charged manganese porphyrin probe (MnPyP), negatively charged aptamer probe, VEGF interaction releases MnPyP probe to catalyze CL reaction.	50 pM	0–25 nM	[143]
Chemiluminescence	VEGF		0.2 pM	1 pM–20 nM	[144]

Table 2 (continued)

Method	Biomarker	Strategy	LOD	Range	Ref.
(signal-off)		T7 Exo-assisted cycling signal amplification/G-quadruplex/hemin DNAzyme, CdS: Eu NCs as luminescent particles, quenching due to G-quadruplex/ hemin/DNAzyme and CdS: Eu NCs complex formation upon VEGF interaction.			
Fluorescence (signal-off)	VEGF	$NaYF_4$:Yb^{3+}, Er^{3+} UCNPs luminescence assay, emission upon UCNP-aptamer complex formation, blocked complex formation under VEGF existence.	6 pM	50 pM–2 nM	[60]
Fluorescence (signal-on)	VEGF	Microchip electrophoresis aptamers were used as electrophoresis mobility modulators for electrophoretic separation, as well as fluorescence affinity probe for fluorescence detection, SYBR-AuNPs as a fluorescent dye, FRET.	2.48 nM	5–150 nM	[130]
Fluorescence (signal-on)	VEGF	Fluorogenic hydrocyanine/quinone reporter pairs, lipid-stabilized nanodroplet association, red fluorescence obtained by addition of VEGF, accumulation of droplets, oxidation of pre-reduced dye with p-fluoranil.	100 fM	100 fM–10 pM	[126]
Fluorescence Enzymatic Amplification (signal-on)	VEGF	DNA assembly structure switching and enzymatic isothermal amplification, fluorescent/quencher-labeled probe. The biosensing platform consists of an aptamer DNA, a primary DNA, a protective DNA, and a template DNA that forms the DNA assembly. After the addition of VEGF, it induces aptamer structure switching and performs an enzymatic isothermal amplification reaction to produce ssDNA.	130 fM	185 fM–15 pM	[21]
Fluorescence (signal-on)	VEGF	Peptide nucleic acid (PNA)-based bound/free separation system, NeutrAvidin beads, fluorescein-labeled aptamer.	25 nM	5–50 nM	[145]
Fluorescence (signal-on)	VEGF	Sandwich aptamer microarray, two fluorescent probe-carrying aptamers, ternary complex formation.	50 nM	NR	[127]
Fluorescence (signal-off)	VEGF	Peroxidase-like activity/Apt–Au NPs/BiOCl nanocomposites, Amplex Red to fluorescein resorufin reaction with H_2O_2, aptamer-VEGF complex induced catalytic activation reduction.	0.5 nM	NR	[20]
Fluorescence Enzymatic Cleavage (signal-on)	VEGF	GO-based FRET nano-aptasensor, endonuclease, analyte-triggered cleavage, weak aptamer affinity to GO sheets, GO acting as a quencher, VEGF interaction results in fluorescent-labeled aptamer fragments release to achieve signal.	1 pM	5–200 pM	[108]
Fluorescence Enzymatic Amplification (signal-on)	VEGF	GO quencher, nano-aptasensor using enzyme-assisted target-recycling signal amplification.	1 pM	5–200 pM	[14]
Fluorescence (signal-off)	VEGF	AuNPs, fluorescence quenching, aptamer, localized surface plasmon resonance, imaging	1.25 pM	1.25 pM–1.25 μM	[97]
Fluorescence FPA	VEGF	G-quadruplex aptamer, VEGF-triggered fluorescence polarization change, analyte-triggered complex formation results in a polarization signal increase.	0.32 nM	0.32–5 nM	[129]
Chemiluminescence (signal-on)	VEGF	A series of different strategies including FRET, CRET, CdSe/ZnS QDs, and black hole quencher pair, QDs-hemin/G-quadruplex supramolecular structure and Exo III-based amplification (please refer to the original paper for further consideration).	5 pM (the lowest)	10 pM–100 nM	[107]
Fluorescence (signal-on)	VEGF	Target-induced structure switching, CuNCs, self-assembly induced emission, and aggregation-induced emission.	12 pM	10–800 pM	[146]
Fluorescence (signal-on)	VEGF	GO quencher, fluorescein dye-labeled aptamer, FRET	0.30 nM	0.5–100 nM	[133]
Chemiluminescence Sandwich Enzymatic (signal-on)	VEGF	Dual-aptamer-based sandwich assay, 4-methoxy-4-(3-phosphatephenyl)-spiro-(1,2-dioxetane-3,2-adamantane) as CL substrate, streptavidin-coated magnetic beads (MBs), alkaline phosphatase.	37 fM	37 fM–740 pM	[112]
Fluorescence (signal-on)	VEGF	Surface-enhanced fluorescence/LSPR using AuNPs, nanoplasmonic fluorophore interaction, poly-L-lysine-coated AuNPs, Cy3B-conjugated aptamers, deactivation of surface plasmon due to fluorescent probe separation in the presence of VEGF.	1.25 pM	1.25 pM– 1.25 μM	[97]

* *NR* not reported.

determination was performed in the range of 0.25–10 nM [96].

Freeman et al. have reported a series of aptasensor-based fluorescence approaches for VEGF detection [107]. This is a comprehensive analysis of various fluorescence approaches using aptamer-based detection where six different (some of them include step-by-step improvement) of them have been reported. One of them was a FRET-based sensor that involves the VEGF-induced separation of aptamer-functionalized quantum dots blocked by a quencher nucleic acid (1 nM LOD). The second strategy that they suggested was another FRET-based sensor using a VEGF-induced assembly of the aptamer subunits functionalized with QDs and a dye acceptor (Cy5) (12 nM LOD). The third strategy was a chemiluminescence aptasensor based on VEGF-induced assembly of a hemin/G-quadruplex catalyst (18 nM LOD), which is similar to another strategy where a chemiluminescence aptasensor based on the VEGF-stimulated assembly of two aptamer subunits into the hemin/G-quadruplex catalyst has been reported (2.6 nM LOD). In this comprehensive study, a chemiluminescence resonance energy transfer (CRET) aptasensor was also reported based on the VEGF-induced assembly of a semiconductor QDs-hemin/G-quadruplex supramolecular structure (875 pM LOD). Then, the analytical performance of the VEGF sensor was improved further using an amplified optical aptasensor system based on the Exo III recycling of the VEGF analyte, and QDs and a black hole quencher as pairs (5 pM LOD).

In the fluorescent polarization analysis (FPA) method, polarized emission from excited molecules is measured after the fluorescent molecules are excited with polarized light [57]. The increase in polarization signal by binding of the target molecule provides a rapid and quantitative analysis in the determination of breast cancer biomarkers [39]. This method has been successfully adapted to the G-quadruplex aptamer-VEGF interaction principle. In the study carried out by Wang et al., a simple method with 320 pM LOD value was developed using a single fluorescent dye attached to the aptamer [129]. The G-quadruplex aptamer-VEGF complex caused a significant change in the polarization signal and VEGF determination could be performed in the range of 0.32–5 nM.

Another nanomaterial type used in fluorescence-based approaches is upconversion nanoparticles (UCNPs) which are alternative fluorophores that convert near-infrared radiation to visible radiation [157, 158]. In a study in which UCNPs were used as a fluorescence tag, a sensor operating in the linear detection range of 50–2000 pM was reported when the VEGF-aptamer complex coupled to the signal probe formed the UCNP-aptamer complex. In this study, 6 pM LOD value was obtained using $NaYF_4$: Yb^{3+}, Er^{3+} UCNPs [60].

Graphene oxide (GO) is a promising nanomaterial due to its unique electrical and optical properties [108, 159]. In fluorescent-based strategies, GO is used for increasing sensitivity and reducing background signals due to its superquenching properties [160]. In studies that use the superquencher feature of GO, sensors with close analytical performances, such as detection limit, have been reported. In an aptasensor study using GO in HER2 detection, a sensor has been developed that can operate in the determination range of 1.2–240 nM and provides 0.96 nM LOD value [133]. A similar principle was reported that a sensor is capable of operating in a wide range of analyte concentrations (40 nM–10 μM) and having a detection limit of 28 nM for MUC1 determination [134].

In a study where GO was utilized with carbon dots as a fluorophore, the FRET sensor developed for MUC1 determination provided a detection limit of 17.1 nM in the 20.0–804.0 nM detection range [135]. In addition to these improvements, in a VEGF assay study using the enzyme-assisted target-recycling signal amplification principle with GO, a low detection limit of 1 pM LOD value was reached in the 5–200 pM assay range [14]. It appears that the principles of target-triggered enzymatic signal amplification are frequently used in biomarker determination and provide LOD values at pM level. Moreover, in a different approach using the endonuclease and cleavage strategy, the analysis was performed using the absorption affinity principle of the VEGF aptamer on the quencher GO nanosheet. In this study, quenching was eliminated by separating the complexes formed in the presence of VEGF into two fragments using an enzymatic way, and 1 pM LOD value was obtained [108].

Magnetic nanoparticles or beads (MNPs or MBs) are also preferable in fluorescence strategies because of their operational advantages such as separation and signal amplification [161]. In chemiluminescence-based VEGF sensor, using a dual-aptamer-based sandwich assay, 4-methoxy-4-(3-phosphatephenyl)-spiro-(1,2-dioxetane-3,2-adamantane) as CL substrate, streptavidin-coated magnetic beads (MBs), and alkaline phosphatase (ALP), 37 fM LOD value was achieved. In that study, VEGF-triggered ALP-catalyzed chemiluminescence reaction was performed as a result of the formation of the aptamer-VEGF-aptamer sandwich on the surface of MBs as illustrated in Fig. 1 [112]. In another study using MB, carbon nanotubes (CNTs), and a fluorescent-labeled aptamer, 38 nM LOD values in the range of 50–250 nM in the HER2 determination were obtained with MB-CNT-aptamer hybrids [116].

Another strategy encountered for the determination of breast cancer biomarkers is the use of AuNPs. In a study using aptamer-conjugated AuNPs on bismuth oxychloride (BiOCl) nanosheets, the production of fluorescent resorufin was achieved in the presence of H_2O_2 with high peroxidase-like activity in the absence of VEGF. VEGF was determined with 0.5 nM LOD value due to decreased signal emission and inhibition of the catalytic activity of the nanocomposite in the

presence of VEGF [20]. In a VEGF sensor using AuNPs with the quenching strategy, 1.25 pM LOD value was reported in a wide determination range of 1.25 pM–1.25 μM [97]. In a HER2 sensor using AgNCs, a "signal-on" sensor was proposed using the principle that the AgNCs conjugated aptamer sequence should be free-form in the folding of complementary bases at both ends in the presence of HER2. In this technique involving this anti-HER2 aptamer and another aptabeacon, a low LOD value of 90.4 aM was obtained [132].

Fluorescence-based aptasensors can also be developed using nanodots (NDs). In one of these FRET strategies, using the carbon NDs with a size of ~ 2 nm that display strong blue-green intrinsic fluorescence, 17.1 nM MUC1 detection limit was achieved [135]. In addition to this approach, antibody-MUC1 and aptamer-MUC1 sandwich structures were used, and a 2 nM LOD value in a wide determination range of 5–100 nM in a quenching-based fluorescent sensor was also reported [136]. In a FRET sensor using a structure switching aptamer, 1.52 nM MUC1 LOD value was reported with the "signal-on" principle using SiNDs [138].

To improve the analytical performances of the fluorescence-based sensors, various strategies have been applied. In a study, Pasquardini et al. developed a chemiluminescence "signal-on" sensor with high sensitivity using a single-photon avalanche diode method, and they reported a 2.15 pM detection limit. In this sensor using an enzymatic approach with HRP and sandwich assay strategy, the analysis was performed on the SiO_2 surface [86]. In general, aptamers were frequently used as aptabeacons in a FRET format in the strategy of detecting biomarkers with fluorescent methods [116, 120, 132–134]. Furthermore, analyte-triggered enzymatic cleavage or primer application strategy was also studied frequently [139, 140, 144]. These analyte-triggered enzymatic reaction-based chemiluminescence strategies often resulted in extremely low detection limits in the range of aM–fM. For example, one of the most sensitive studies was performed using an immuno-loop-mediated isothermal amplification assay (Im-LAMP) illustrated in Fig. 2. In this study, ultrasensitive detection of MUC1 was achieved with an LOD value of 1 aM using aptamer-based Im-LAMP strategy. Moreover, aptasensors, including nanomaterials such as GO, CNDs, SiNDs, AgNCs, and QD, have also proven that analytical performance can be enhanced by providing both broad detection range and low detection limits.

Colorimetric and plasmonic-based detection strategies

Colorimetric-based detection strategies are preferred due to their ease of use and allowing PoC applications [162, 163]. The principle of colorimetric strategies is to determine the presence of target analytes with the color change without the need for any measuring device where AuNPs are generally used for color change-based detection [164]. The response of surface electrons to an external electromagnetic excitation in AuNPs is known as local surface plasmon resonance (LSPR). This resonance changes by the media contacting the surface of the AuNP or as a result of aggregation, and consequently the color of the colloid changes. Enzymatic or sandwich aptasensors using direct dyes as well as LSPR are used in the determination of biomarkers for breast cancer. In Table 3, a comparison of the strategies and analytical performances used by colorimetric aptasensors for VEGF, MUC1, and HER2 is given.

In a study where AuNPs were used as colorimetric signals, 10 nM LOD value was obtained using a lateral flow assay and HER2 binding aptamers. This PoC approach was able to operate within the detection range of 10–100 nM HER2. In another study in which AuNPs were used as colorimetric markers, the signal was obtained by the release of AuNPs into the solution as a result of the enzymatic reaction. Aptazyme, obtained by combining the aptamer with DNAzyme, can provide DNAzyme activation as a result of molecular recognition between the aptamer and its target. In a study using this approach, the binding of the hairpin aptamer to VEGF was performed to convert the colorless molecule to green dye in the presence of H_2O_2 and hemin after G-quadruplex DNAzyme production and 1.70 pM LOD value was obtained [163]. A similar approach was also reported for MUC1 detection using magnetic nanoparticles (MNPs). In the study using trivalent peroxidase-mimic G-quadruplex DNAzyme and magnetic nanoparticles, MUC1 was determined as a result of H_2O_2-mediated oxidation of dye. A 5.08 nM LOD value was reported with this sensor, which can perform MUC1 detection in a wide detection range of 50 nM–1 μM [166]. Instead of obtaining a dye as a result of a reaction, a study aimed at obtaining a signal with color change as a result of the agglomeration of AuNPs using the method mentioned above was also published by Wu et al. [15]. In this study, a hairpin structure consisting of DNAzyme and a short stem sequence was developed. In this sensor, DNAzyme was activated in the presence of VEGF, separated the linkers attached to the AuNPs, causing red color. With this approach, 0.1 nM LOD value has been reported (0.1–40 nM range).

Hybridization chain reaction (HCR) is an enzyme-free amplification process performed under isothermal conditions [152]. In a study using a nonlinear HCR strategy, a colorimetric VEGF sensor was reported using the interaction between dendritic DNA structures with the probe-stabilized AuNPs and hairpin probe in the presence of VEGF. This sensor was used for VEGF determination with 0.18 nM LOD value in the 0–7.4 nM detection range [152].

Plasmonic-based strategies use the electron-associated phenomena called plasmon that takes place on metal nanostructures [172]. A detailed review article has recently been

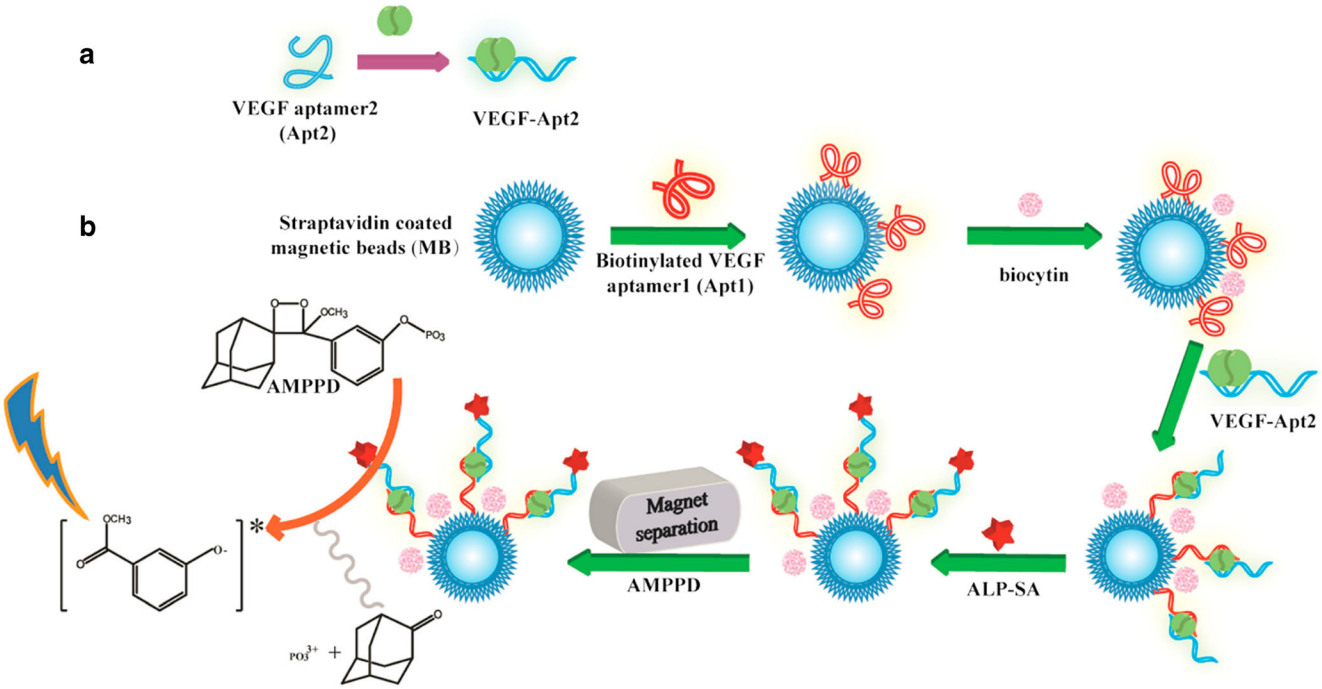

Fig. 1 Schematic representation of the dual-aptamer-based sandwich assay using aptamer immobilization on magnetic beads following by ALP-catalyzed CL reaction for highly sensitive detection of VEGF. **a** Representing the incubation of VEGF165 sample with aptamer solution. **b** Illustrates the immobilization of aptamer on magnetic beads and coupling with VEGF aptamer for CL detection. Reproduced from ref. [112]

published on the analytical performances of plasmonic biosensors and the approaches used in their production [173]. SPR is one of the label-free approaches for measuring ligand-analyte interactions [68, 74]. These types of sensors measure the change in the properties of electromagnetic waves that occur due to the interaction between the analyte and molecular probe on the sensor surface [169, 174]. SPR technology can be used in biosensing utilizing nanofilms of noble metals in the detection of biomarkers [174, 175].

Different analytical strategies and nanomaterials were used by various research groups to increase the analytical performance of plasmonic-based aptasensors in biomarker detection. In a study using dopamine-coated gold nanorods immobilized onto the micro-grooving PDMS substrates, 34 pM LOD value was obtained for HER2 in the 34–204 nM detection range [168]. However, to increase the relatively weak analytical performance, 1 pM LOD value was obtained for VEGF with the sandwich assay approach which was successfully applied in other strategies. In this enhanced-performance approach, the SPR signal was improved using the aptamer-protein-antibody complex and an antibody-conjugated HRP enzyme [169]. In another VEGF aptasensor in a microfluidic format, aptamer sequences were synthesized in situ using the surface transcription reaction of the T7 RNA polymerase; thereby, signal amplification was performed [170]. Since the purpose of this study is to demonstrate that transcription can be used in sensor applications, the determination was performed using 40 nM VEGF, but no LOD or detection interval analytical parameter was reported. Another SPR strategy was proposed by the same research group for VEGF determination using rolling circle amplification, an isothermal enzymatic technique for replication of ssDNAs, where a LOD value of 3.7 pM was obtained [171]. In a study where the direct aptamer-VEGF relationship was examined with SPR, but a simpler assembly was used for the SPR platform, 0.8 nM LOD value was reported for Au nanofilm-coated plastic optical fiber [85].

In surface-enhanced Raman scattering (SERS), which is a powerful spectroscopic technique, highly sensitive detections can be performed by increasing Raman signals with AuNPs [167, 176]. Gold and silver nanoparticles are SERS-active materials due to their plasmonic properties [177]. Especially hollow or multi-sided forms of plasmonic nanomaterials are widely used in SERS-based detection methods [178]. In a VEGF sensor developed with this approach, the AgNP-decorated AuNPs pyramid structure providing a strong SERS signal was used [167]. In this sensor, VEGF was detected with 22.6 aM LOD value as a result of SERS signal decrease with aptamer-VEGF interaction as illustrated in Fig. 3. The VEGF detection range of this sensor was, on the other hand, relatively narrow (0.01–1.0 fM). In another study, an approach was attempted to increase the sensor determination range to 3.7 fM–37 nM VEGF [87]. Silica-encapsulated hollow gold nanospheres, VEGF antigen sandwich assay, and a gold-patterned microarray were used in this SERS-based

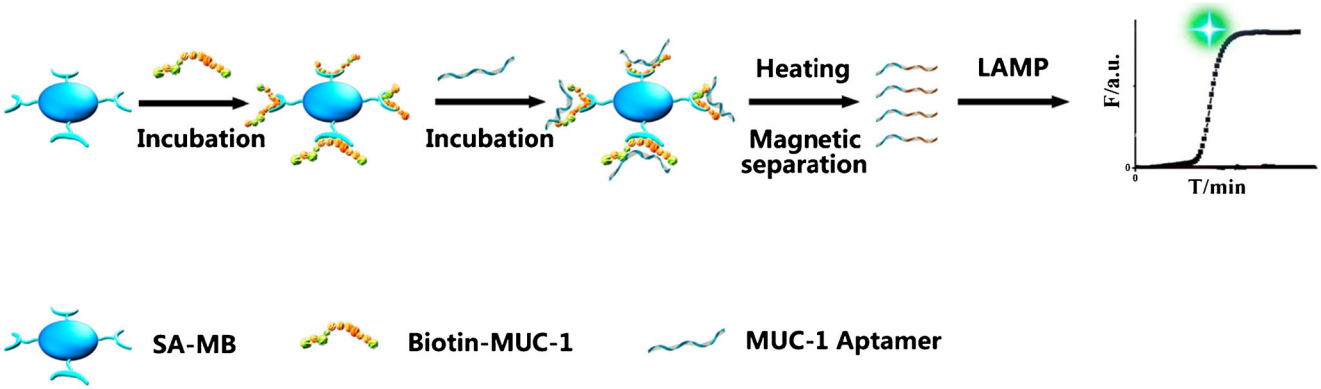

Fig. 2 Schematic representation of an aptamer-based immuno-loop-mediated isothermal amplification assay using MUC1 aptamer for highly ultrasensitive detection of MUC1 molecules. Reproduced from ref. [121]

sandwich immunoassay strategy. VEGF could be detected with a sandwich assay and a signal-on approach with a 37 fM LOD value.

It would be expected that SPR-based sensor strategies, which were successfully used in the diagnosis of many other analytes, would be supported by more studies. Toxin and pathogen analysis from food samples [179, 180] and studies on various areas such as veterinary practices [181], pharmaceutical industry [182], and other medical diagnosis applications [183] were performed using SPR. In the coming years, the use of aptamer and different nanotechnological signal enhancement strategies, and the use of SPR in the determination of biomarkers in the diagnosis of breast cancer, could be of interest as other SPR-based studies. Furthermore, despite its successful results at the detection limit, there are also a few aptasensor studies on SERS-based breast cancer biomarker diagnosis. It seems that there is a need for the development of both SPR and SERS-based detection strategies using aptamers on cancer biomarkers.

Electrochemical strategies

Electrochemical biosensors operate based on detecting the electrical signal produced after specific binding of biomaterials such as aptamer, enzyme, antibody, or nucleic acids on the surface of a metal or carbon electrode, or after catalytic reactions [184, 185]. Electrochemical biosensors are widely used for biomedical analysis and early detection or monitoring of diseases [186]. Table 4 summarizes the electrochemical techniques that have been used for the determination of breast cancer biomarkers [216].

Impedimetric techniques

Electrochemical impedance spectroscopy (EIS) is one of the most commonly used electrochemical methods due to its low excitation voltage, fastness, and high sensitivity. Due to the low excitation voltage, EIS is more suitable for long-term and real-time detection. Zhou et al. reported a 1.7 fM detection limit for HER2 using an impedimetric aptasensor with a bimetallic MnFe Prussian blue analog coupled to AuNPs, gold electrode, and ferrocene (Fc). HER2 analysis in living MCF-7 cells and human serum was performed within the range of 6.8 fM–6.8 pM [191]. It is stated that the developed aptasensor is selective, acceptably reproducible, stable, and well applicable for the detection of HER2 and live MCF-7 cells in human serum.

In an aptasensor study, 550 fM LOD value was obtained for HER2 analysis using tetrahedral DNA nanostructure HER2-specific aptamer as recognition probes and flower-like nanozymes/horseradish peroxidase (HRP) as signal nanoprobes. In this sandwich assay, HER2 determination was performed in the determination range of 690 fM–690 pM using Mn_3O_4/Pd@Pt/HRP-based nanoprobe and gold electrode [187]. Another aptasensor developed by direct aptamer immobilization on the gold disc electrode; however, a lower analytical performance was obtained (34 pM LOD) [42]. HER2 aptasensor, which has the best analytical performance among the sensors using the EIS technique in the electrochemical detection of breast cancer biomarkers, has recently been reported by Rostamabadi. In this study, the glassy carbon electrode (GCE) was modified by adding densely packed AuNPs to the electrochemically reduced graphene oxide and single-walled carbon nanotube composite as illustrated in Fig. 4. The HER2 sensor showed a low detection limit of 340 aM and was successfully used for the detection of HER2 from serum samples [188]. A label-free electrochemical aptasensor based on ordered mesoporous carbon–gold nanocomposite modified screen-printed electrode (SPE) has been fabricated for the detection of VEGF [73]. In this study, 50 fM LOD value was obtained with the EIS technique.

Another impedimetric method, the non-Faradaic EIS (nFIS), has been used to detect both HER2 and VEGF from breast cancer biomarkers. An nFIS sensor developed by immobilizing the anti-HER2 aptamer directly on the

Table 3 Colorimetric and plasmonic strategies for VEGF, HER2, and MUC1 aptasensors

Method	Biomarker	Strategy	LOD	Range	Ref.
Colorimetric (signal-off)	HER2	Lateral flow assay, HER2 binding aptamers, and AuNPs	10 nM	10–99 nM	[165]
Colorimetric Enzymatic (signal-on)	MUC1	Trivalent peroxidase-mimicking DNAzyme and magnetic nanoparticles, G-quadruplex DNA-hemin complex, DNAzyme catalyzed H_2O_2-mediated oxidation of ABTS dye (blue-green product),	5.08 nM	50–1000 nM	[166]
Colorimetric Enzymatic (signal-on)	VEGF	Strand displacement amplification, hairpin aptamer, G-quadruplex DNAzyme, DNAzyme catalyzed H_2O_2-mediated oxidation of ABTS dye (blue-green product),	1.70 pM	24 pM–11.25 nM	[163]
Colorimetric Enzymatic (signal-off)	VEGF	AuNPs/target-induced activation of aptazyme, crosslinked AuNPs, G-quadruplex DNAzyme	0.1 nM	0.1–40 nM	[15]
Colorimetric Enzymatic Amplification	VEGF	AuNPs/target-assisted cascade amplification, nonlinear HCR, DNA dendrimers, color change due to agglomeration.	185 pM	0–7.4 nM	[152]
SERS Sandwich	VEGF	SERS-based sandwich immunoassay using silica-encapsulated hollow gold nanospheres and VEGF antigen sandwich assay and a gold-patterned microarray, signal-on.	37 fM	3.7 fM–37 nM	[87]
SERS	VEGF	SERS active, AgNP-decorated AuNP pyramids, aptamer-conjugated AgNPs, signal-off	22.6 aM	0.01–1.0 fM	[167]
SPR	HER2	Dopamine-coated Au nanorods immobilized onto the micro-grooving PDMS substrates, HER2-specific aptamers.	34 pM	34–204 nM	[168]
SPR Enzymatic	VEGF	RNA aptamer/protein biomarker/HRP-conjugated antibodies sandwich structure, HRP catalyzed, sandwich assay	1 pM	NR	[169]
SPR Enzymatic Amplification	VEGF	On-chip synthesis/RNA aptamer microarray/microfluidic format, T7 RNA polymerase, enzymatic amplification, imaging SPR	NR	NR	[170]
SPR Enzymatic Amplification	VEGF	Carboxyl-coated polystyrene microbeads, rolling circle amplification (an isothermal enzymatic DNA replication process)	3.7 pM	4 pM–40 nM	[171]
SPR	VEGF	Plastic optical fiber, Au film, SPR	3 nM	NR	[85]

interdigitated gold electrode, HER2 determination from undiluted serum was performed in the range of 1 pM–100 nM. The detection limit obtained using this sensor was 1 pM [190]. With a similar approach, the determination of HER2 from dilute human serum was performed between 1.4 and 14 pM [189]. A hybrid aptamer–antibody-based sandwich analysis was also reported by Qureshi et al. and determination of VEGF performed from a real serum sample in the 250 fM–50 pM determination range with a 20 fM LOD value [192].

Voltammetric techniques

Voltammetry is another electro-analytical method in which the current is measured by sweeping the potential such as

cyclic voltammetry (CV), differential pulse voltammetry (DPV), and square wave voltammetry (SWV). SWV and DPV are often used among different voltammetry methods, due to their high sensitivity and fast response. It is also widely used for the detection of cancer biomarkers in several different configurations.

As a result of the shape change or preferential bonding that occurs when the aptamers interact with their targets, the release approach of the second weakly linked reporter sequence is frequently used in electrochemical sensors. These target-triggered approaches have been successfully applied in the detection of VEGF, MUC1, and HER2 biomarkers. In one of these approaches, there is a sandwich assay where the aptamer was used as both a molecular diagnostic element and a signal-generating reporter. HER2 detection was performed on the gold electrode in the range of 6.8–680 fM and a 0.32 fM LOD value was reported [195]. In a study using the aptamer switching approach, VEGF detection was performed in 3 different cancer cell lines. In this study, a very low detection limit (7.5 pM) was obtained with voltammetric measurements on the gold electrode [208]. In an SPE based on alternating current voltammetry (ACV) study, the target-induced conformational change of the aptamer was used and VEGF detection was performed with a detection limit of 5 pM in whole blood [61]. Liu et al. developed an SWV-based aptasensor that uses a target-triggered redox tag release approach to detect MUC1. This aptasensor was used to detect MUC1 simultaneously with the carcinoembryonic antigen with a detection limit of 130 pM MUC1 in the detection range of 10–100 nM on the gold electrode [200]. In a sensor using dual signal-tagged (methylene blue and ferrocene) hairpin structured DNA-based aptasensor, GCE and AuNPs to increase the signal, MUC1 was determined with a detection limit of 827 pM [201]. The detection ranges in this aptasensor using the SWV technique was relatively wide, ranging from 1 nM to 1 μM. Other target-triggered switching and probe release approaches used in MUC1 detection showed a relatively poor analytical performance. For example, an SWV aptasensor with DNA hairpin-switching technique has a 4 nM LOD value [202], whereas a DPV based aptasensor with AuNPs and enzyme signal amplification has a 2.2 nM LOD value [53].

An immuno-hybrid sandwich assay was recently developed by Jarczewska et al. In this study, gold disc electrodes were modified with antibody-methylene blue labeled aptamer hybrid layer and HER2 detection was performed with a detection limit of 6.8 pM in a slightly narrow determination range (6.8–68 pM) with the target trigger release [196]. In a study using a similar detection strategy, VEGF was detected by applying both EIS and DPV techniques. Bovine serum albumin (BSA) -gold nanoclusters / ionic liquid and glassy carbon

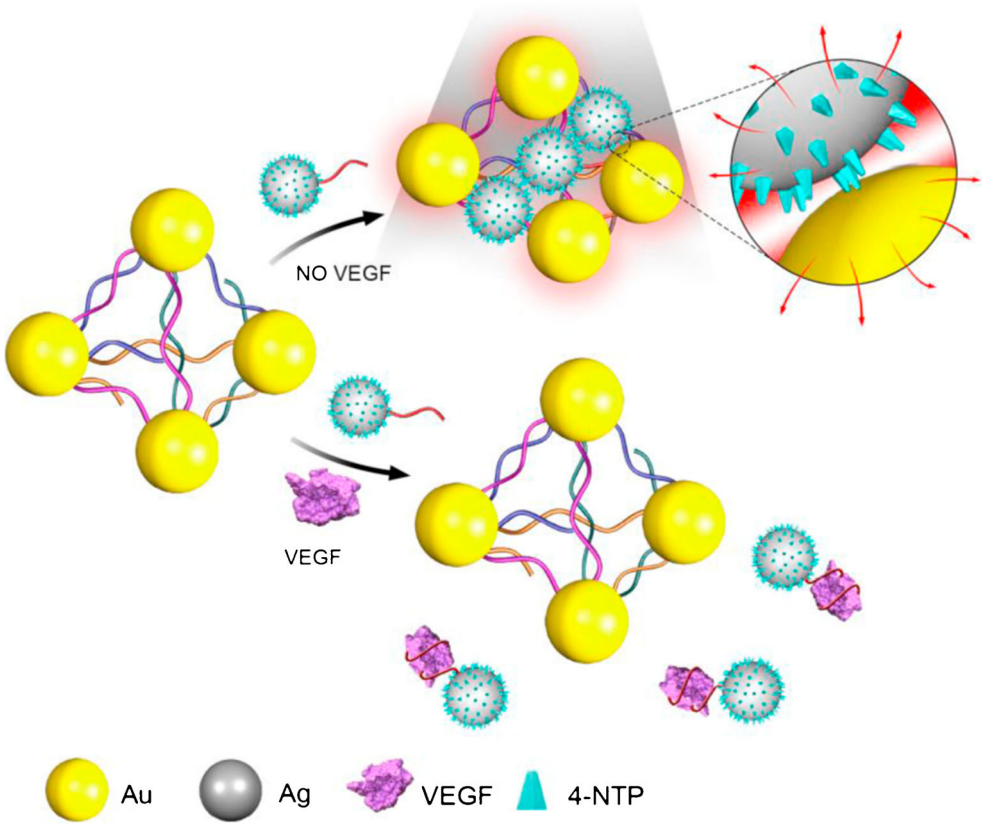

Fig. 3 Schematic representation of SERS-based detection of VEGF using AgNP-decorated AuNP pyramid structure providing a strong SERS signal. Highly selective and ultrasensitive detection of VEGF was developed. Reproduced from ref. [167]

electrode were used resulting 0.32 pM LOD value with DPV while 0.48 pM LOD value was obtained with EIS [213].

Enzymatic signal amplification and target-triggered amplification strategies were also preferred to further improve the detection limit. In one of these approaches, Nonaka et al. developed a sandwich assay, where they labeled the VEGF-binding aptamer with pyrroloquinoline quinone glucose dehydrogenase and immobilized the other aptamer on gold wire electrode. This approach was used in VEGF detection with a detection limit of 15 nM [113]. However, as an alternative to this enzymatic assay, whose analytical performance is somewhat low, VEGF detection was performed with DPV with 320 fM LOD value by developing an amplification strategy with the use of target-triggered cycloaddition reaction [212]. The cycloaddition reaction carried out between alkyne- modified aptamer and the azide functionalized electrode surface with the help of copper catalyst by applying cathodic potential has provided a detection range of 1–120 pM, nevertheless, it gives a low detection limit value. Since simultaneous amplification strategies with the analysis can be very successful, another study using cyclic target-induced primer extension reaction, aptamer-hairpin probe, and enzyme-amplified electrochemical readout approach was applied to achieve 30 fM LOD value. This DPV-based aptasensor was used in complex biological matrices to determine VEGF in the detection range of 37 fM −37 pM [209].

Using the target-induced probe release strategy together with nanomaterials positively affects the analytical performance of the biomarker sensor. Wang et al. recently developed a competitive electrochemical where cDNA-ferrocene/(Ti_3C_2) nanosheets were used as a probe, and the result of the target-triggered release of the probe was able to detect MUC1 in a fairly wide detection range (1.0 pM–10 μM) [205]. Using the SWV technique on GCE, MUC1 detection was performed with a detection limit of 330 fM [205].

In a study, the analytical performance of the electrochemical sensor was increased using nanomaterials, and MUC1 detection with 31 aM LOD value was performed using AuNPs and graphene oxide-doped poly(3,4-ethylene dioxythiophene) as shown in Fig. 5. In this sensor using the DPV technique, MUC1 was detected from human serum samples on the fluorine tin oxide (FTO) glass sheet substrate in the detection range of 3.13 aM–31.25 nM [203]. This LOD value provides the best analytical performance among the electrochemical strategies in this review article. Other studies using carbon-based nanomaterial, although not as high as the previous study, still provided good analytical performance. Yang et al. reached 250 fM LOD value in MUC1 detection on GCE with a three-dimensional graphene-based ratiometric signal amplification aptasensor. Operating in a fairly wide range (1 pM–1 μM), this aptasensor used the Au-rGO composite to improve analytical performance [204]. In VEGF detection, 0.7 pM LOD value was obtained using the DPV technique using rGO-poly(amidoamine)/Au nanocomposite and thionine [214]. In this study, cytochrome c and VEGF detection were performed simultaneously using dual aptasensor and SPE. In a HER2 assay using reduced graphene oxide-chitosan film, 1.4 pM LOD value was reported [197].

In another voltammetric sensor study using carbon nanomaterials-based strategies, a 1.85 pM VEGF detection limit was achieved using the graphene oxide/aptamer, Au-electrode, and poly-L-lactide nanoparticles for signal amplification approach [159]. Chen et al. reported MUC1 detection with a 1 pM LOD value in a sandwich assay using a dual signal amplification strategy. Thionine was used as an electrochemical probe in this study where poly(o-phenylenediamine)-AuNP hybrid film was used as a carrier, and AuNP-functionalized silica/multiwalled carbon nanotube core-shell nanocomposites as tracing tag [111].

Another approach to improve analytical performance is the use of magnetic beads. In a recent study, Malecka et al. performed HER2 detection with a detection limit of 1 fM and a detection range of 10 fM–100 pM using the aptasensor they developed using a sandwich assay and magnetic bead [193]. In a study using magnetic beads for MUC1 detection, 0.07 nM LOD value was obtained using sandwich assay and DPV [199]. There is also a study on improving the voltammetric sensor response using bimetallic nanoclusters. In a study, VEGF detection was performed in the range of 6–20 pM using the peroxidase-mimicking activity feature of aptamer-conjugated Ag/Pt bimetallic nanoclusters [30]. A 4.6 pM LOD value was obtained with human serum samples. In a sandwich assay-based study in which different nanostructures are used in HER2 voltammetric aptasensor, gold nanorod@Pd superstructures/aptamer/horseradish peroxidase was used as a signal probe, DNA-quadruplex was used as a molecular recognition element, and HER2 determination was performed with a detection limit of 1 pM in a wide detection range (68 pM–1.36 nM) [194]. CV-based VEGF aptasensor was also reported in a wide determination range (100 fM–10 nM) using graphitic carbon nitride (g-C_3N_4) as photoactive material. Working on the target-triggered methylene blue release, this sensor provided 30 fM LOD value [210].

Field-effect transistor-based techniques

Field-effect transistors (FETs) are based on the immobilization of the molecular sensing element on a semiconductor line between the source and drain electrodes. In the transistor structure, the varying channel conductivity is measured as a result of the interaction of the analyte with the molecular diagnostic element by modulating the gate electrode [217]. In the n-type FET system, when the molecular diagnostic element interacts with the positively charged analyte, the conductivity increases, and if it interacts with the negatively charged

Table 4 Electrochemical strategies for VEGF, HER2, and MUC1 aptasensors

Method	Biomarker	Strategy	LOD	Range	Ref.
Impedimetric EIS	HER2	Single-stranded DNA aptamer self-assembled onto the monolayer of 3-mercaptopropionic acid on AuNP-modified gold disc electrode	34 pM 5 ng/mL	34–680 pM	[42]
Impedimetric EIS Sandwich	HER2	Tetrahedral DNA nanostructure HER2-specific aptamer as recognition probes and flower-like nanozymes/horseradish peroxidase (HRP) as signal nanoprobes, Mn_3O_4/Pd@Pt/HRP-based nanoprobe, gold electrode	550 fM	690 fM–690 pM	[187]
Impedimetric EIS	HER2	AuNPs placed on a composite consisting of electrochemically reduced graphene oxide and single-walled carbon nanotubes, GCE	340 aM	0.68 fM–6.87 pM	[188]
Impedimetric nFIS	HER2	Interdigitated gold electrodes, thiol-terminated DNA aptamer	NR ~1.4 pM	1.4–14 pM	[189]
Impedimetric nFIS	HER2	Interdigitated gold electrodes, thiol-terminated DNA aptamer	1 pM	1 pM–100 nM	[190]
Impedimetric EIS	HER2	Bimetallic MnFe Prussian blue analog coupled to AuNPs, gold electrode, Fc	1.7 fM	6.8 fM–6.8 pM	[191]
Impedimetric EIS	VEGF	Mesoporous carbon–Au nanoparticle-decorated SPE, aptamer	0.05 pM	0.5–15 pM	[73]
Impedimetric nFIS	VEGF	Aptamer–antibody-based sandwich assay, antibody-conjugated magnetic beads,	20 fM	250 fM–50 pM	[192]
Voltammetric Chronocoulometry Sandwich	HER2	Cellulase-linked sandwich assay on magnetic beads, aptamer-conjugated magnetic beads, cellulase-labeled aptamer, graphite electrode	1 fM	10 fM–100 pM	[193]
Voltammetric DPV Sandwich	HER2	Gold nanorod@Pd super- structure aptamer-horseradish peroxidase as the signal probe, DNA-quadruplex as molecular recognition element, gold electrode	1 pM	68 pM–1.36 nM	[194]
Voltammetric SWV Sandwich	HER2	Aptamer as molecular recognition element and signal-generating reporter, sandwich format, target-triggered self-assembly, molybdate reaction, gold electrode	0.32 fM	6.8–680 fM	[195]
Voltammetric SWV Sandwich	HER2	Gold disk electrodes modified with antibody-methylene blue labeled aptamer hybrid layer, methylene blue redox label, target-triggered release	6.8 pM	6.8–68 pM	[196]
Voltammetric DPV	HER2	Reduced graphene oxide-chitosan film, methylene blue, SPE	1.4 pM	3.4–510 pM	[197]
Voltammetric Conductimetric	MUC1	Single polypyrrole nanowire-based microfluidic aptasensor, conduction	2.66 nM	2.66–66.5 nM	[198]
Voltammetric DPV Sandwich	MUC1	Streptavidin or Protein G-modified magnetic beads, sandwich format, labeled secondary aptamer, alkaline phosphatase enzyme (1-naphthyl phosphate)	0.07 nM	0–0.28 nM	[199]
Voltammetric DPV	MUC1	Target-triggered hairpin oligonucleotide switch, AuNPs, enzyme signal amplification, HRP, o-phenylenediamine catalytic reaction with H_2O_2, SPE	2.2 nM	8.8–353.3 nM	[53]
Voltammetric SWV	MUC1	DNA linker containing anti-MUC1 aptamer, conjugated with methylene blue as redox tag, target-triggered release, gold electrode	0.13 nM	10–100 nM	[200]
Voltammetric SWV	MUC1	Dual signal-tagged hairpin structured DNA-based ratiometric probe, ferrocene-labeled signal probe and methylene blue-modified inner reference probe, AuNPs, GCE	0.827 nM	1 nM–1 μM	[201]
Voltammetric SWV	MUC1	DNA hairpin containing anti-MUC1 aptamer, conjugated with methylene blue as redox tag, target-triggered release, gold electrode	4 nM	4–680 nM	[202]
Voltammetric DPV	MUC1	AuNPs and graphene oxide-doped poly(3,4-ethylenedioxythiophene), FTO glass sheets	31 aM	3.13 aM–31.25 nM	[203]
Voltammetric ACV	MUC1	Three-dimensional graphene-based ratiometric signal amplification aptasensor, Au-rGO composite, Fc-labeled aptamer, GCE	0.25 pM	1 pM–1 μM	[204]
Voltammetric SWV	MUC1	Competitive electrochemical aptasensor based on a cDNA-ferrocene/(Ti_3C_2) nanosheets, target-triggered release of cDNA-Fc/(Ti_3C_2) nanosheet probe, GCE	0.33 pM	1 pM–10 μM	[205]
Voltammetric DPV Sandwich	MUC1	Dual signal amplification strategy, poly(o-phenylenediamine)-AuNP hybrid film as a carrier, AuNP-functionalized silica/multiwalled carbon nanotube core-shell nanocomposites as tracing tag, electrochemical probe thionine	1 pM	1–100 nM	[111]
Voltammetric DPV	VEGF	SPE decorated with Au nanoparticles, graphite screen-printed electrodes, signal amplification via an enzyme catalyzed the hydrolysis of the electroinactive 1-naphthyl phosphate to 1-naphthol, sandwich assay	30 nM	0–250 nM	[206]

Table 4 (continued)

Method	Biomarker	Strategy	LOD	Range	Ref.
Voltammetric DPV	VEGF	Graphene oxide/aptamer, Au-electrode, poly-L-lactide nanoparticles for signal amplification	1.85 pM	1.85 pM–3.7 nM	[159]
Voltammetric DPV	VEGF	Hemin, sandwich assay, aptamer	1 nM	0–80 nM	[207]
Voltammetric ACV	VEGF	Target-induced conformational change/methylene blue-modified aptamer, gold-coated SPE electrode	5 pM	50 pM–0.15 nM	[61]
Voltammetric SWV	VEGF	Self-assembly of thiolated aptamers on gold electrode, methylene blue as redox label, aptamer switching, tested in three prostate cell lines (RWPE-1, LNCaP, and PC3)	7.5 pM	7.5 pM–5 nM	[208]
Voltammetric DPV Amplification	VEGF	Cyclic target-induced primer extension, aptamer-hairpin probe and enzyme-amplified electrochemical readout	30 fM	37 fM–37 pM	[209]
Voltammetric CV Photoelectrochemical	VEGF	Graphitic carbon nitride (g-C_3N_4) as photoactive material, aptamer-bridged DNA network structure, MB electron transport through the DNA helix structure, suppressing the recombination of electron-hole pairs generated by g-C_3N_4, target-triggered methylene blue release	30 fM	100 fM–10 nM	[210]
Voltammetric	VEGF	Magnetic beads, bound/free separation system, hybridization capacity changes with capture DNA immobilized on beads in the presence or absence of target molecules	~ 10 nM	10 nM–1 μM	[211]
Voltammetric Sandwich Amplification	VEGF	Sandwich method/ pyrroloquinoline quinone glucose dehydrogenase/enzymatic signal amplification, gold wire electrode.	15 nM	15–60 nM	[113]
Voltammetric EIS DPV Amplification	VEGF	Electrochemically triggered click (amplification) reaction by adjusting the applied cathodic potential, copper catalyst, cycloaddition reaction between the alkyne-modified aptamer and the azide-functionalized electrode surface, gold electrode	6.2 nM 0.32 pM	0–10 μM 1–120 pM	[212]
Voltammetric DPV EIS	VEGF	BSA-gold nanoclusters/ionic liquid, GCE electrode, target-induced desorption of methylene blue probe from aptamer (for DPV), target-induced mass-transfer limitation Fc (for EIS)	0.32 pM 0.48 pM	1–120 pM 2.5–250 pM	[213]
Voltammetric DPV	VEGF	rGO-poly(amidoamine)/Au nanocomposite as supporting matrix for covalent immobilization of thionine, anti-VEGF aptamer, SPE dual working electrode, simultaneous detection of cytochrome c and VEGF	0.7 pM	2.5–320 pM	[214]
Voltammetric CV	VEGF	Ag/Pt bimetallic nanoclusters, aptamer-Ag/Pt NCs have intrinsic peroxidase-mimicking activity, catalytic, H_2O_2-mediated oxidation of a substrate, TMB	4.6 pM	6–20 pM	[30]
Voltammetric pH meter Amplification	VEGF	Immuno-hybridization chain reaction (HCR), an enzyme-free amplification process, target VEGF- antibody-aptamer sandwich structure, GOx-functionalized ssDNA	18.5 fM	30 fM–18 pM	[32]
Voltammetric Glucose meter Amplification	VEGF	Immuno-HCR, invertase-functionalized auxiliary probe, VEGF-triggered hybridization chain reaction to generate invertase-concatemers, invertase-catalyzed sucrose to glucose.	44 fM	110 fM–3.6 pM	[31]
FET (p-type)	VEGF	Few layer graphene, poly(pyrrole) as source material, FET, nitrogen-doped graphene (p-type), RNA aptamer	100 fM	100 fM–10 nM	[110]
FET (p-type)	VEGF	Carboxyl-functionalized poly(pyrrole) nanotube, FET, DNA aptamer	0.4 pM	400 fM–10 nM	[125]
FET (p-type) (n-type)	VEGF	n-type and p-type silicon nanowire, methylated RNA aptamer	n-type: 1.04 n-M p-type: 104 p-M	100–52 pM	[215]

analyte, the conductivity decreases. On the other hand, the opposite is the case for p-type FET [218]. Kwon et al. performed VEGF determination with a p-type FET sensor where carboxylated polypyrrole nanotubes were used as the gate electrode. This FET sensor operated in a fairly wide detection range (400 fM–10 nM) and reached a LOD value of 0.4 pM in VEGF determination [125]. In another study conducted by the same group, a FET-type VEGF aptasensor using nitrogen-doped several layer graphenes was also reported. In this study, VEGF determination provided a more successful detection

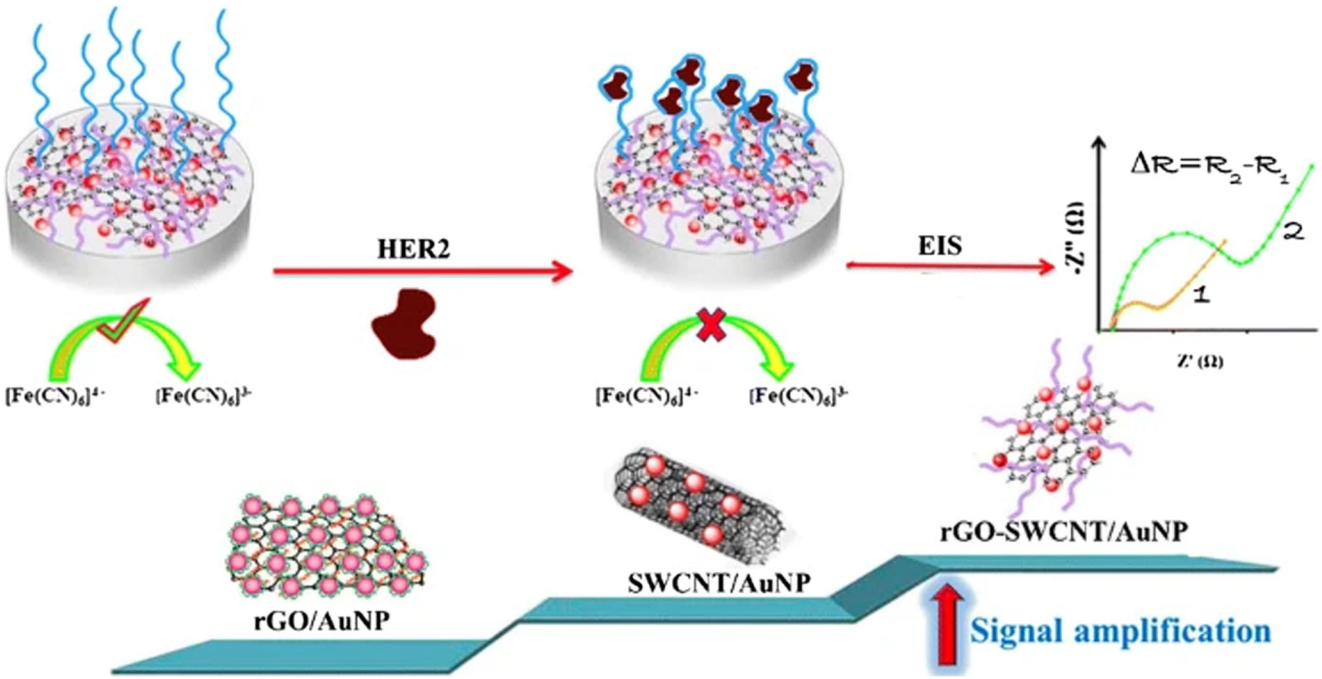

Fig. 4 Schematic representation of the sensitive detection of HER2 using densely packed AuNP-reduced graphene oxide and single-walled carbon nanotube composite. The impedimetric sensor developed has a LOD value of 340 aM and successfully tested with serum samples. Sera of breast cancer patients were differentiated from the sera of healthy persons. Reproduced from ref. [188]

limit with 100 fM LOD compared with the previous study. However, the operating range of the reported sensor was between 100 fM and 10 nM, similar to the previous study result [110]. In a study, a FET aptasensor was developed using an aptamer-immobilized n-type and p-type Si nanowire (SiNW) gate. Using this aptasensor, VEGF was accurately detected for n-type and p-type SiNW-FETs with a LOD of 1.04 nM and 104 pM, respectively [215]. Although the number of FET-based aptasensor studies used for the diagnosis of breast cancer is limited, the FET strategy is widely used for the determination of other analytes. A detailed review article recently published on this subject can be accessed [219].

Other electrochemical techniques

Two different approaches were also seen in the electrochemical analysis. One of these approaches aimed to perform VEGF determination using a pH meter. Xu et al. reported an aptamer-antibody sensor using a sandwich structure. In this study, the target VEGF was first captured by the antibody immobilized on the microplate and bound with an aptamer to form the sandwich structure. Then, with the help of ssDNA with GOx, a hybridization chain reaction took place, so that GOx catalyzed the oxidation of glucose and caused a pH change. VEGF detection was carried out in a detection range of 30 fM–18 pM with a limit of 18.5 fM [32]. With a similar approach, in a VEGF sensing strategy using an immuno-hybridization chain reaction, the conventional glucometer was used to obtain a 44 fM detection limit which was achieved in the 110 fM–3.6 pM detection range. This very low detection limit, obtained using a personal glucose meter, worked on the principle of catalyzing sucrose to glucose using an invertase auxiliary probe that triggers the hybridization chain reaction to produce invertase-concatemers [31].

Other methods and commercial kits

In this section, the results of VEGF, HER2, and MUC1 analysis reported in the literature using chromatographic strategies and commercial ELISA methods are compared. Antibody-based assays such as ELISA are the only commercial detection kits available for VEGF, HER2, and MUC1 [97, 167]. Compared with aptasensors, antibody-based assays have many disadvantages, such as the following: (1) their applicable targets are limited to immunogenic response, (2) their production is time-consuming and costly, (3) their poor stability due to sensitivity to pH and temperature, and (4) their modification is expensive and difficult [220]. However, analytical performances of ELISA methods are satisfactory and meet clinical criteria. Table 5 summarizes the detection limits and the ranges of ELISA methods compared with other strategies.

Aptamers, on the other hand, have been frequently used in VEGF, MUC1, and HER2 analysis especially due to their various advantages performing similar to ELISA kits.

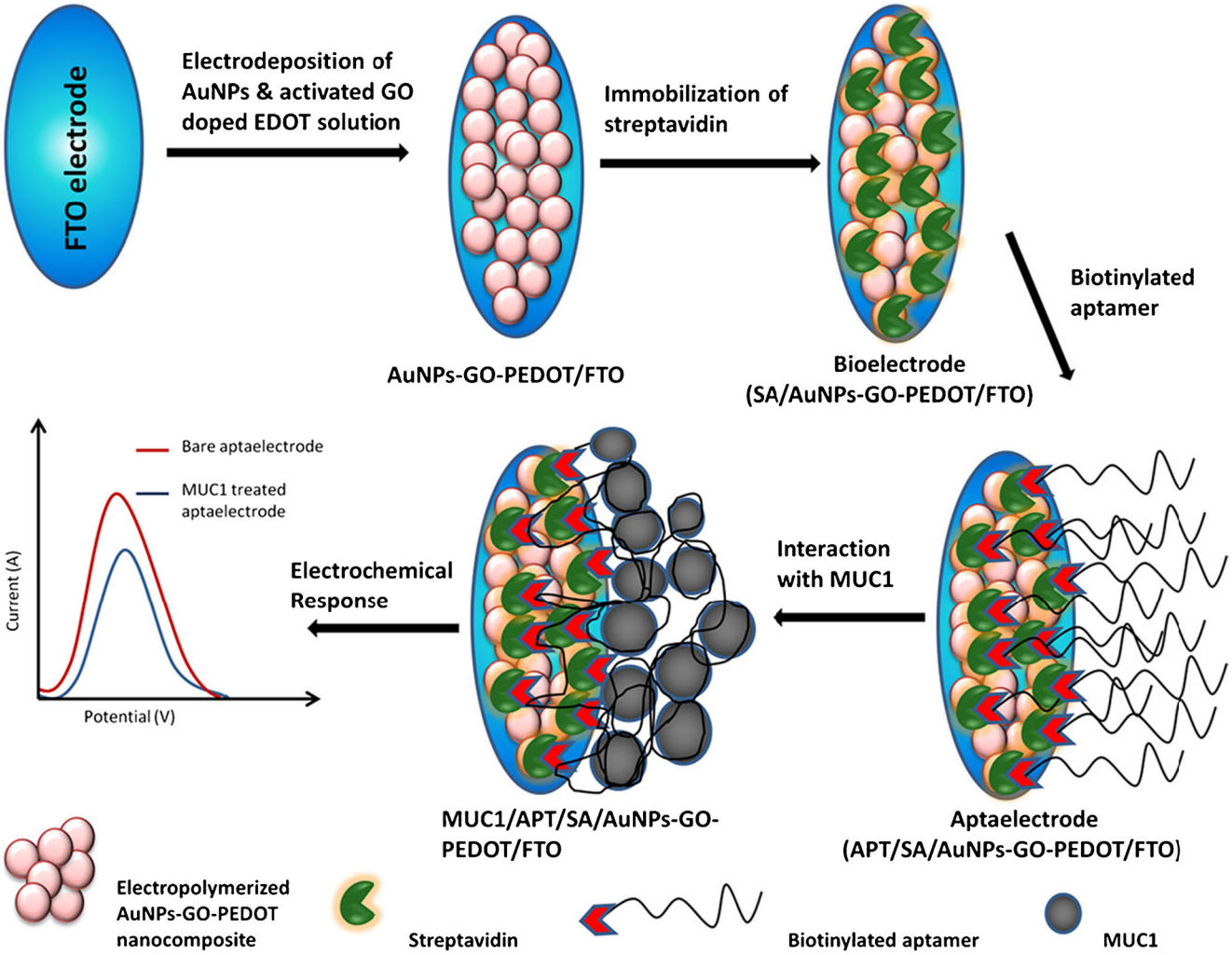

Fig. 5 Schematic representation of an ultrasensitive detection of MUC1 AuNPs and graphene oxide-doped poly(3,4-ethylenedioxythiophene) nanocomposite. FTO sheet was used as an electrode and the DVP technique was utilized. The developed sensor showed good stability, reusability, and successfully tested in serum samples. Reproduced from ref. [203]

Besides, liquid chromatography-tandem mass spectrometry approaches can provide a very low detection limit (25 pM) [221, 222]. However, the strategies discussed in this article have proved to be as sensitive as to existing methods providing simple analytical approaches and low-cost analysis with adequate analytical performance.

In this review article, since extensive studies have been carried out using aptamers, it is impossible to cover all of them. For example, using atomic force microscopy, the interaction force of the aptamer with VEGF was measured by single-molecule force spectroscopy and found to be 169.44 ± 6.59 pN and this value was found to be compatible with k_d value [225]. Molecularly imprinted polymers (MIP) are also used such as monomers of acrylamide and N, N′-methylene bis(acrylamide)-based electrochemical sensor was reported for VEGF detection with 0.005 pg/mL LOD and 0.01–7000 pg/mL range [226]. HER2 detection also reported electrochemical MIP on a gold electrode, and 1.6 ng/mL determination limit was obtained in the range of 10–70 ng/mL [227]. Finally, unlike the strategies within the scope of this review article, there is another strategy based on microcantilever detection of MUC1 reported in recent years. The measurements carried out by immobilizing thiol modified anti-MUC1 aptamers in the form of self-assembled monolayers on the microcantilever, and detection in the range of 5–500 nM was obtained with 0.9 nM detection limits [223].

Conclusions and future perspectives

In recent years, aptamer-based biosensors with different strategies have been preferred for accurate and rapid detection of cancer biomarkers. The unique properties of aptamers compared with antibodies allow them to be used as a molecular

Table 5 Comparison of some commercial ELISA kits and chromatographic methods for VEGF, MUC1, and HER2 analysis

Method	Target	Approach	LOD	Range	Ref.
Liquid chromatography--tandem mass spectrometry	HER2	Quasi-targeted proteomics assay converted the HER2 signal into the mass response of reporter peptide by a combination of aptamer-peptide probe and LC-MS/MS.	25 pM	25 pM–2.5 nM	[221]
Ultraperformance liquid chromatography--tandem mass spectrometry	VEGF	Acquity UPLC BEH C18 chromatography column, gradient elution using acetonitrile and 0.1% formic acid as the mobile phase. Positive multiple reaction monitoring modes.	37 pM	37 pM–37 nM	[222]
Microcantilever	MUC1	With thiolated aptamers of MUC1 self-assembled on the sensing microcantilever, MUC1 interacts with aptamers resulting in the change of surface stress on the microcantilever.	0.9 nM	5–500 nM	[223]
ELISA	MUC1	Commercial kit	800 nM	NR	[120]
ELISA	MUC1	Commercial kit	0.065 nM	15 pM–10 nM	[121]
ELISA	VEGF	Commercial kit	0.18 pM	0.18–0.74 pM	[97]
ELISA	HER2	Commercial kit	4.29 pM	4.29–275 pM	[224]

diagnostic element in a wide range of biomarker detection platforms. One of the major advantages of aptamers is that they are suitable for chemical modifications and conjugation with different labels or active molecules [228].

In this review article, aptasensors that use different strategies were discussed for VEGF, HER2, and MUC1 detection. Selected aptamer sequences and their affinities reported in the literature are compared in Table 1 in which VEGF stands out as the most utilized biomarker using aptamers for multiple detection strategies. Although RNA aptamers have enhanced affinities, DNA-based aptamers were often used in biomarker detection strategies [78, 184]. DNA-based aptamers are used to increase the analytical performance of the sensors along with nanomaterials. The unique properties of nanomaterials have led to the integration of the sensor with the different strategies to ensure that the signal received from the transducer is sensitive and reliable. The relevant literature involves an increasing number of studies to improve the analyte performance of sensors integrating several nanomaterials into different sensor platforms. Among various metal NPs, AuNPs are indispensable for fluorescence chemiluminescence-based, colorimetric, electrochemical, and plasmonic sensor strategies. In addition to the large surface area provided by AuNPs, it has other advantages such as unique optic and electrical properties, high stability, controllable morphology, biocompatibility, and easy functionality with known methods. Moreover, carbon-based nanomaterials (graphene, nanotube, etc.) have been used in many detection strategies to increase analytical performance. Carbon-based nanomaterials function as super-quencher or fluorophores in fluorescence-based strategies and as electron transfer enhancer in electrochemical strategies.

There are many studies for the detection of biomarkers as specified in this review article recently, and these strategies do not make it to the market as commercial products. One of the reasons for this is the use of conservative approaches in the

diagnosis of cancer such as biopsy or the preference of golden methods in the detection of biomarkers such as chromatography [229] . However, this review article reveals that almost all of the aptasensors developed using various strategies can provide clinical analysis requirements. Moreover, some of these strategies proposed herein even include the use of platforms suitable for PoC. These strategies also meet the requirements expected from the biosensor such as the ability to analyze with a small amount of sample, resistance to interference, one-step analysis, unlabeled analysis, and ease of use.

Although each method reviewed in this paper has several advantages, there are considerable down points based on different applications and end-user needs. For example, optical methods are often quite promising since sensitive results can be obtained; however, there are important drawbacks that one should consider before picking a suitable strategy. For example, fluorescent and chemiluminescence-based methods must be performed in the lab environment; therefore, if PoC testing is needed at clinics and medical centers without lab infrastructure, this strategy would not be suitable, regardless of how sensitive results can be achieved. Furthermore, there is also a stability issue with fluorescent molecules over time, which is a process called photobleaching, that can affect the long-term usability of developed sensors. Another optical-based strategy, colorimetric biosensors, was not as often preferred in the literature because they have high detection limits compared with other methods, therefore, fail to meet the required criteria for biomarker detection. On the other hand, plasmonic sensors can achieve low detection limits as low as aM range; however, high-cost equipment and trained personnel are needed for analysis. That is why the studies for both colorimetric and plasmonic biosensors are limited in the literature. Finally, electrochemical sensors seem to be the most promising biomarker detection strategy among all others. The electrochemical-based biosensors are not only competitive with fluorescent and chemiluminescence-based methods for the detection of biomarkers but also the most suitable strategy for PoC testing. Moreover, the electrochemical tests are rapid, easy, and do not require complex sample preparation and equipment. All strategies benefit certain improvements in which electrochemical methods stand out to be the best candidate for on-site and/or rapid analysis. There are quite a remarkable number of biosensor studies that can be found in the literature among all detection strategies especially for VEGF and MUC1 biomarkers. On the other hand, the biosensor studies for HER2 biomarker for this detection strategy are quite limited. In terms of obtaining significant analytical performance, enzymatic amplification strategies stand out with the lowest detection limits reported as low as aM concentrations. Also, popular strategies such as the use of nanomaterials stand out for signal amplification.

Furthermore, instead of identifying a biomarker alone, multiple biomarker identification simultaneously can prevent false diagnosis ratios. In this case, however, the following problems should be addressed: (1) a clear consensus has not been established for most of the cancer diagnosis since cancer biomarker research is still evolving [230, 231]; (2) the difficulties of the development of multi-biomarker detection devices, which often require multidisciplinary research projects [232]; (3) more specific aptamers are still needed to be developed and integrated into sensor platforms (4); and the development of cheap and reliable sensor platforms is needed for continuous monitoring during cancer progression. Consequently, it will not be a surprise that we come across an increasing number of studies on the development of aptasensors for the detection of biomarkers using different strategies focusing on the mentioned problems in the coming years.

Compliance with ethical standards

Conflict of interest The authors declare that they have no competing interests.

References

1. Siegel RL, Miller KD, Jemal A (2019) Cancer statistics, 2019. CA Cancer J Clin 69(1):7–34. https://doi.org/10.3322/caac.21551
2. Henley SJ, Ward EM, Scott S, Ma J, Anderson RN, Firth AU, Thomas CC, Islami F, Weir HK, Lewis DR, Sherman RL, Wu M, Benard VB, Richardson LC, Jemal A, Cronin K, Kohler BA (2020) Annual report to the nation on the status of cancer, part I: national cancer statistics. Cancer 126(10):2225–2249. https://doi.org/10.1002/cncr.32802
3. DeSantis CE, Fedewa SA, Goding Sauer A, Kramer JL, Smith RA, Jemal A (2016) Breast cancer statistics, 2015: convergence of incidence rates between black and white women. CA Cancer J Clin 66(1):31–42. https://doi.org/10.3322/caac.21320
4. DeSantis C, Ma J, Bryan L, Jemal A (2014) Breast cancer statistics, 2013. CA Cancer J Clin 64(1):52–62. https://doi.org/10.3322/caac.21203
5. Torre LA, Bray F, Siegel RL, Ferlay J, Lortet-Tieulent J, Jemal A (2015) Global cancer statistics, 2012. CA Cancer J Clin 65(2):87–108. https://doi.org/10.3322/caac.21262
6. Liu M, Li Z, Yang J, Jiang Y, Chen Z, Ali Z, He N, Wang Z (2016) Cell-specific biomarkers and targeted biopharmaceuticals for breast cancer treatment. Cell Prolif 49(4):409–420. https://doi.org/10.1111/cpr.12266
7. Azim HA, Ibrahim AS (2014) Breast cancer in Egypt, China and Chinese: statistics and beyond. J Thorac Dis 6(7):864–866. https://doi.org/10.3978/j.issn.2072-1439.2014.06.38
8. Nover AB, Jagtap S, Anjum W, Yegingil H, Shih WY, Shih W-H, Brooks AD (2009) Modern breast cancer detection: a technological review. International Journal of Biomedical Imaging 2009: 902326. https://doi.org/10.1155/2009/902326
9. Prabhakar B, Shende P, Augustine S (2018) Current trends and emerging diagnostic techniques for lung cancer. Biomed Pharmacother 106:1586–1599. https://doi.org/10.1016/j.biopha.2018.07.145
10. Mittal S, Kaur H, Gautam N, Mantha AK (2017) Biosensors for breast cancer diagnosis: a review of bioreceptors, biotransducers

and signal amplification strategies. Biosens Bioelectron 88:217–231. https://doi.org/10.1016/j.bios.2016.08.028
11. Hayes B, Murphy C, Crawley A, O'Kennedy R (2018) Developments in point-of-care diagnostic technology for cancer detection. Diagnostics (Basel, Switzerland) 8(2):39. https://doi.org/10.3390/diagnostics8020039
12. Florea A, Taleat Z, Cristea C, Mazloum-Ardakani M, Săndulescu R (2013) Label free MUC1 aptasensors based on electrodeposition of gold nanoparticles on screen printed electrodes. Electrochem Commun 33:127–130. https://doi.org/10.1016/j.elecom.2013.05.008
13. Siegel RL, Miller KD, Jemal A (2015) Cancer statistics, 2015. CA Cancer J Clin 65(1):5–29. https://doi.org/10.3322/caac.21254
14. Li X, Ding X, Fan J (2015) Nicking endonuclease-assisted signal amplification of a split molecular aptamer beacon for biomolecule detection using graphene oxide as a sensing platform. Analyst 140(23):7918–7925. https://doi.org/10.1039/c5an01759a
15. Wu D, Gao T, Lei L, Yang D, Mao X, Li G (2016) Colorimetric detection of proteins based on target-induced activation of aptazyme. Anal Chim Acta 942:68–73. https://doi.org/10.1016/j.aca.2016.09.010
16. Altintas Z, Tothill I (2013) Biomarkers and biosensors for the early diagnosis of lung cancer. Sensors Actuators B Chem 188:988–998. https://doi.org/10.1016/j.snb.2013.07.078
17. Greenberg DA, Jin K (2004) Experiencing VEGF. Nat Genet 36(8):792–793. https://doi.org/10.1038/ng0804-792
18. Olsson A-K, Dimberg A, Kreuger J, Claesson-Welsh L (2006) VEGF receptor signalling ? In control of vascular function. Nat Rev Mol Cell Biol 7(5):359–371. https://doi.org/10.1038/nrm1911
19. Goel HL, Mercurio AM (2013) VEGF targets the tumour cell. Nat Rev Cancer 13(12):871–882. https://doi.org/10.1038/nrc3627
20. Hsu C-L, Lien C-W, Wang C-W, Harroun SG, Huang C-C, Chang H-T (2016) Immobilization of aptamer-modified gold nanoparticles on BiOCl nanosheets: tunable peroxidase-like activity by protein recognition. Biosens Bioelectron 75:181–187. https://doi.org/10.1016/j.bios.2015.08.049
21. Li J, Sun K, Chen Z, Shi J, Zhou D, Xie G (2017) A fluorescence biosensor for VEGF detection based on DNA assembly structure switching and isothermal amplification. Biosens Bioelectron 89:964–969. https://doi.org/10.1016/j.bios.2016.09.078
22. Ferrara N (2004) Vascular endothelial growth factor: basic science and clinical progress. Endocr Rev 25(4):581–611. https://doi.org/10.1210/er.2003-0027
23. Simons M, Gordon E, Claesson-Welsh L (2016) Mechanisms and regulation of endothelial VEGF receptor signalling. Nat Rev Mol Cell Biol 17(10):611–625. https://doi.org/10.1038/nrm.2016.87
24. Hoeben A, Landuyt B, Highley MS, Wildiers H, Van Oosterom AT, De Bruijn EA (2004) Vascular endothelial growth factor and angiogenesis. Pharmacol Rev 56(4):549–580. https://doi.org/10.1124/pr.56.4.3
25. Carmeliet P, Jain RK (2000) Angiogenesis in cancer and other diseases. Nature 407(6801):249–257. https://doi.org/10.1038/35025220
26. Salven P, Orpana A, Joensuu H (1999) Leukocytes and platelets of patients with cancer contain high levels of vascular endothelial growth factor. Clin Cancer Res 5(3):487–491
27. Ray D, Mishra M, Ralph S, Read I, Davies R, Brenchley P (2004) Association of the VEGF gene with proliferative diabetic retinopathy but not proteinuria in diabetes. Diabetes 53(3):861–864. https://doi.org/10.2337/diabetes.53.3.861
28. Nakahara H, Song J, Sugimoto M, Hagihara K, Kishimoto T, Yoshizaki K, Nishimoto N (2003) Anti-interleukin-6 receptor antibody therapy reduces vascular endothelial growth factor production in rheumatoid arthritis. Arthritis Rheum 48(6):1521–1529. https://doi.org/10.1002/art.11143
29. Detmar M (2004) Evidence for vascular endothelial growth factor (VEGF) as a modifier gene in psoriasis. J Invest Dermatol 122(1):xiv–xv. https://doi.org/10.1046/j.0022-202X.2003.22140.x
30. Fu X-M, Liu Z-J, Cai S-X, Zhao Y-P, Wu D-Z, Li C-Y, Chen J-H (2016) Electrochemical aptasensor for the detection of vascular endothelial growth factor (VEGF) based on DNA-templated Ag/Pt bimetallic nanoclusters. Chin Chem Lett 27(6):920–926. https://doi.org/10.1016/j.cclet.2016.04.014
31. Zhu X, Kou F, Xu H, Lin L, Yang G, Lin Z (2017) A highly sensitive aptamer-immunoassay for vascular endothelial growth factor coupled with portable glucose meter and hybridization chain reaction. Sensors Actuators B Chem 253:660–665. https://doi.org/10.1016/j.snb.2017.06.174
32. Xu H, Kou F, Ye H, Wang Z, Huang S, Liu X, Zhu X, Lin Z, Chen G (2017) Highly sensitive antibody-aptamer sensor for vascular endothelial growth factor based on hybridization chain reaction and pH meter/indicator. Talanta 175:177–182. https://doi.org/10.1016/j.talanta.2017.04.073
33. Roskoski R Jr (2007) Vascular endothelial growth factor (VEGF) signaling in tumor progression. Crit Rev Oncol Hematol 62(3):179–213. https://doi.org/10.1016/j.critrevonc.2007.01.006
34. Yarden Y (2001) The EGFR family and its ligands in human cancer: signalling mechanisms and therapeutic opportunities. Eur J Cancer 37(Suppl 4):S3–S8. https://doi.org/10.1016/s0959-8049(01)00230-1
35. Liu M, Yu X, Chen Z, Yang T, Yang D, Liu Q, Du K, Li B, Wang Z, Li S, Deng Y, He N (2017) Aptamer selection and applications for breast cancer diagnostics and therapy. Journal of nanobiotechnology 15(1):81–81. https://doi.org/10.1186/s12951-017-0311-4
36. Lukong KE (2017) Understanding breast cancer-the long and winding road. BBA Clin 7:64–77. https://doi.org/10.1016/j.bbacli.2017.01.001
37. Toss A, Cristofanilli M (2015) Molecular characterization and targeted therapeutic approaches in breast cancer. Breast Cancer Res 17:60. https://doi.org/10.1186/s13058-015-0560-9
38. Maleki S, Dorokhova O, Sunkara J, Schlesinger K, Suhrland M, Oktay MH (2013) Estrogen, progesterone, and HER-2 receptor immunostaining in cytology: the effect of varied fixation on human breast cancer cells. Diagn Cytopathol 41(10):864–870. https://doi.org/10.1002/dc.22973
39. Wu M, Ma J (2017) Association between imaging characteristics and different molecular subtypes of breast cancer. Acad Radiol 24(4):426–434. https://doi.org/10.1016/j.acra.2016.11.012
40. Slamon DJ, Clark GM, Wong SG, Levin WJ, Ullrich A, McGuire WL (1987) Human breast cancer: correlation of relapse and survival with amplification of the HER-2/neu oncogene. Science 235(4785):177–182. https://doi.org/10.1126/science.3798106
41. Slamon DJ, Godolphin W, Jones LA, Holt JA, Wong SG, Keith DE, Levin WJ, Stuart SG, Udove J, Ullrich A et al (1989) Studies of the HER-2/neu proto-oncogene in human breast and ovarian cancer. Science 244(4905):707–712. https://doi.org/10.1126/science.2470152
42. Chun L, Kim S-E, Cho M, W-s C, Nam J, Lee DW, Lee Y (2013) Electrochemical detection of HER2 using single stranded DNA aptamer modified gold nanoparticles electrode. Sensors Actuators B Chem 186:446–450. https://doi.org/10.1016/j.snb.2013.06.046
43. Zhang J, Liu Y (2008) HER2 over-expression and response to different chemotherapy regimens in breast cancer. J Zhejiang Univ Sci B 9(1):5–9. https://doi.org/10.1631/jzus.B073003
44. Musolino A, Ciccolallo L, Panebianco M, Fontana E, Zanoni D, Bozzetti C, Michiara M, Silini EM, Ardizzoni A (2011) Multifactorial central nervous system recurrence susceptibility in patients with HER2-positive breast cancer: epidemiological and clinical data from a population-based cancer registry study. Cancer 117(9):1837–1846. https://doi.org/10.1002/cncr.25771

45. Rouanet P, Roger P, Rousseau E, Thibault S, Romieu G, Mathieu A, Cretin J, Barneon G, Granier M, Maran-Gonzalez A, Daures JP, Boissiere F, Bibeau F (2014) HER2 overexpression a major risk factor for recurrence in pT1a-bN0M0 breast cancer: results from a French regional cohort. Cancer Med 3(1):134–142. https://doi.org/10.1002/cam4.167
46. Wu X, Shaikh AB, Yu Y, Li Y, Ni S, Lu A, Zhang G (2017) Potential diagnostic and therapeutic applications of oligonucleotide aptamers in breast cancer. Int J Mol Sci 18(9). https://doi.org/10.3390/ijms18091851
47. Marin F, Luquet G, Marie B, Medakovic D (2007) Molluscan shell proteins: primary structure, origin, and evolution. In: current topics in developmental biology, vol 80. Academic Press, pp 209–276. doi: https://doi.org/10.1016/S0070-2153(07)80006-8
48. Lakshmanan I, Ponnusamy MP, Macha MA, Haridas D, Majhi PD, Kaur S, Jain M, Batra SK, Ganti AK (2015) Mucins in lung cancer: diagnostic, prognostic, and therapeutic implications. J Thorac Oncol 10(1):19–27. https://doi.org/10.1097/JTO.0000000000000404
49. Roy LD, Sahraei M, Subramani DB, Besmer D, Nath S, Tinder TL, Bajaj E, Shanmugam K, Lee YY, Hwang SIL, Gendler SJ, Mukherjee P (2011) MUC1 enhances invasiveness of pancreatic cancer cells by inducing epithelial to mesenchymal transition. Oncogene 30(12):1449–1459. https://doi.org/10.1038/onc.2010.526
50. Rahn JJ, Dabbagh L, Pasdar M, Hugh JC (2001) The importance of MUC1 cellular localization in patients with breast carcinoma:an immunohistologic study of 71 patients and review of the literature. Cancer 91(11):1973–1982. https://doi.org/10.1002/1097-0142(20010601)91:11<1973::AID-CNCR1222>3.0.CO;2-A
51. Ma F, Ho C, Cheng AKH, Yu H-Z (2013) Immobilization of redox-labeled hairpin DNA aptamers on gold: electrochemical quantitation of epithelial tumor marker mucin 1. Electrochim Acta 110:139–145. https://doi.org/10.1016/j.electacta.2013.02.088
52. Liu X, Qin Y, Deng C, Xiang J, Li Y (2015) A simple and sensitive impedimetric aptasensor for the detection of tumor markers based on gold nanoparticles signal amplification. Talanta 132:150–154. https://doi.org/10.1016/j.talanta.2014.08.072
53. Hu R, Wen W, Wang Q, Xiong H, Zhang X, Gu H, Wang S (2014) Novel electrochemical aptamer biosensor based on an enzyme-gold nanoparticle dual label for the ultrasensitive detection of epithelial tumour marker MUC1. Biosens Bioelectron 53:384–389. https://doi.org/10.1016/j.bios.2013.10.015
54. Nath S, Mukherjee P (2014) MUC1: a multifaceted oncoprotein with a key role in cancer progression. Trends Mol Med 20(6):332–342. https://doi.org/10.1016/j.molmed.2014.02.007
55. Moreno M, Bontkes HJ, Scheper RJ, Kenemans P, Verheijen RHM, von Mensdorff-Pouilly S (2007) High level of MUC1 in serum of ovarian and breast cancer patients inhibits huHMFG-1 dependent cell-mediated cytotoxicity (ADCC). Cancer Lett 257(1):47–55. https://doi.org/10.1016/j.canlet.2007.06.016
56. Gheybi E, Amani J, Salmanian AH, Mashayekhi F, Khodi S (2014) Designing a recombinant chimeric construct contain MUC1 and HER2 extracellular domain for prediagnostic breast cancer. Tumor Biol 35(11):11489–11497. https://doi.org/10.1007/s13277-014-2483-y
57. Cruz I, Ciudad J, Cruz JJ, Ramos M, Gomez-Alonso A, Adansa JC, Rodriguez C, Orfao A (2005) Evaluation of multiparameter flow cytometry for the detection of breast cancer tumor cells in blood samples. Am J Clin Pathol 123(1):66–74. https://doi.org/10.1309/wp3qwkvjfydhhxqd
58. Colomer R, Aranda-López I, Albanell J, García-Caballero T, Ciruelos E, López-García MÁ, Cortés J, Rojo F, Martín M, Palacios-Calvo J (2018) Biomarkers in breast cancer: a consensus statement by the Spanish Society of Medical Oncology and the Spanish Society of Pathology. Clinical & translational oncology: official publication of the Federation of Spanish Oncology Societies and of the National Cancer Institute of Mexico 20(7):815–826. https://doi.org/10.1007/s12094-017-1800-5
59. Moelans C, De Weger R, Van der Wall E, Van Diest P (2011) Current technologies for HER2 testing in breast cancer. Crit Rev Oncol Hematol 80(3):380–392
60. Lan J, Li L, Liu Y, Yan L, Li C, Chen J, Chen X (2016) Upconversion luminescence assay for the detection of the vascular endothelial growth factor, a biomarker for breast cancer. Microchim Acta 183(12):3201–3208. https://doi.org/10.1007/s00604-016-1965-6
61. Zhao S, Yang W, Lai RY (2011) A folding-based electrochemical aptasensor for detection of vascular endothelial growth factor in human whole blood. Biosens Bioelectron 26(5):2442–2447. https://doi.org/10.1016/j.bios.2010.10.029
62. Elmore JG, Barton MB, Moceri VM, Polk S, Arena PJ, Fletcher SW (1998) Ten-year risk of false positive screening mammograms and clinical breast examinations. N Engl J Med 338(16):1089–1096. https://doi.org/10.1056/nejm199804163381601
63. Anderson SM, Chen TT, Iruela-Arispe ML, Segura T (2009) The phosphorylation of vascular endothelial growth factor receptor-2 (VEGFR-2) by engineered surfaces with electrostatically or covalently immobilized VEGF. Biomaterials 30(27):4618–4628. https://doi.org/10.1016/j.biomaterials.2009.05.030
64. Prabhulkar S, Alwarappan S, Liu G, Li C-Z (2009) Amperometric micro-immunosensor for the detection of tumor biomarker. Biosens Bioelectron 24(12):3524–3530. https://doi.org/10.1016/j.bios.2009.05.002
65. Suzuki Y, Yokoyama K (2009) Development of a fluorescent peptide for the detection of vascular endothelial growth factor (VEGF). ChemBioChem 10(11):1793–1795. https://doi.org/10.1002/cbic.200900190
66. Lindenberg MA, Miquel-Cases A, Retel VP, Sonke GS, Wesseling J, Stokkel MPM, van Harten WH (2017) Imaging performance in guiding response to neoadjuvant therapy according to breast cancer subtypes: a systematic literature review. Crit Rev Oncol Hematol 112:198–207. https://doi.org/10.1016/j.critrevonc.2017.02.014
67. Turner APF (2013) Biosensors: sense and sensibility. Chem Soc Rev 42(8):3184–3196. https://doi.org/10.1039/C3CS35528D
68. Damborský P, Švitel J, Katrlík J (2016) Optical biosensors. Essays Biochem 60(1):91–100. https://doi.org/10.1042/ebc20150010
69. Hianik T, Wang J (2009) Electrochemical aptasensors–recent achievements and perspectives. Electroanalysis 21(11):1223–1235. https://doi.org/10.1002/elan.200904566
70. Garyfallou G-Z, Ketebu O, Şahin S, Mukaetova-Ladinska EB, Catt M, Yu EH (2017) Electrochemical detection of plasma immunoglobulin as a biomarker for Alzheimer's disease. Sensors 17(11):2464
71. Perumal V, Hashim U (2014) Advances in biosensors: principle, architecture and applications. J Appl Biomed 12(1):1–15. https://doi.org/10.1016/j.jab.2013.02.001
72. Şahin S, Merotra J, Kang J, Trenell M, Catt M, Yu EH (2018) Simultaneous electrochemical detection of glucose and non-esterified fatty acids (NEFAs) for diabetes management. IEEE Sensors J 18(22):9075–9080
73. Amouzadeh Tabrizi M, Shamsipur M, Farzin L (2015) A high sensitive electrochemical aptasensor for the determination of VEGF165 in serum of lung cancer patient. Biosens Bioelectron 74:764–769. https://doi.org/10.1016/j.bios.2015.07.032
74. Fan X, White IM, Shopova SI, Zhu H, Suter JD, Sun Y (2008) Sensitive optical biosensors for unlabeled targets: a review. Anal Chim Acta 620(1):8–26. https://doi.org/10.1016/j.aca.2008.05.022

75. Şahin S (2019) A simple and sensitive hydrogen peroxide detection with horseradish peroxidase immobilized on pyrene modified acid-treated single-walled carbon nanotubes. J Chem Technol Biotechnol
76. Giuliano Z, Roberta L, Fabio G, Tommaso B, Marco B (2017) Emerging applications of label-free optical biosensors. Nanophotonics 6(4):627–645. https://doi.org/10.1515/nanoph-2016-0158
77. Kimoto M, Nakamura M, Hirao I (2016) Post-ExSELEX stabilization of an unnatural-base DNA aptamer targeting VEGF165 toward pharmaceutical applications. Nucleic Acids Res 44(15): 7487–7494. https://doi.org/10.1093/nar/gkw619
78. Ellington AD, Szostak JW (1990) In vitro selection of RNA molecules that bind specific ligands. Nature 346(6287):818–822. https://doi.org/10.1038/346818a0
79. Tuerk C, Gold L (1990) Systematic evolution of ligands by exponential enrichment: RNA ligands to bacteriophage T4 DNA polymerase. Science 249(4968):505–510. https://doi.org/10.1126/science.2200121
80. Fang X, Tan W (2010) Aptamers generated from cell-SELEX for molecular medicine: a chemical biology approach. Acc Chem Res 43(1):48–57. https://doi.org/10.1021/ar900101s
81. Xi Z, Zheng B, Wang C (2016) Synthesis, surface modification, and biolabeling with aptamer of Fe3O4@SiO2 magnetic nanoparticles. Nanosci Nanotechnol Lett 8(12):1061–1066. https://doi.org/10.1166/nnl.2016.2246
82. Keefe AD, Pai S, Ellington A (2010) Aptamers as therapeutics. Nat Rev Drug Discov 9(7):537–550. https://doi.org/10.1038/nrd3141
83. Mayer G (2009) The chemical biology of aptamers. Angew Chem Int Ed Engl 48(15):2672–2689. https://doi.org/10.1002/anie.200804643
84. Xi Z, Huang R, Deng Y, He N (2014) Progress in selection and biomedical applications of aptamers. J Biomed Nanotechnol 10(10):3043–3062. https://doi.org/10.1166/jbn.2014.1979
85. Cennamo N, Pesavento M, Lunelli L, Vanzetti L, Pederzolli C, Zeni L, Pasquardini L (2015) An easy way to realize SPR aptasensor: a multimode plastic optical fiber platform for cancer biomarkers detection. Talanta 140:88–95. https://doi.org/10.1016/j.talanta.2015.03.025
86. Pasquardini L, Pancheri L, Potrich C, Ferri A, Piemonte C, Lunelli L, Napione L, Comunanza V, Alvaro M, Vanzetti L, Bussolino F, Pederzolli C (2015) SPAD aptasensor for the detection of circulating protein biomarkers. Biosens Bioelectron 68:500–507. https://doi.org/10.1016/j.bios.2015.01.042
87. Ko J, Lee S, Lee EK, Chang S-I, Chen L, Yoon S-Y, Choo J (2013) SERS-based immunoassay of tumor marker VEGF using DNA aptamers and silica-encapsulated hollow gold nanospheres. Phys Chem Chem Phys 15(15):5379–5385. https://doi.org/10.1039/C2CP43155F
88. Hofmann HP, Limmer S, Hornung V, Sprinzl M (1997) Ni2+ −binding RNA motifs with an asymmetric purine-rich internal loop and a G-A base pair. Rna 3(11):1289–1300
89. Rajendran M, Ellington AD (2008) Selection of fluorescent aptamer beacons that light up in the presence of zinc. Anal Bioanal Chem 390(4):1067–1075. https://doi.org/10.1007/s00216-007-1735-8
90. Hermann T, Patel DJ (2000) Adaptive recognition by nucleic acid aptamers. Science 287(5454):820–825. https://doi.org/10.1126/science.287.5454.820
91. Bock LC, Griffin LC, Latham JA, Vermaas EH, Toole JJ (1992) Selection of single-stranded DNA molecules that bind and inhibit human thrombin. Nature 355(6360):564–566. https://doi.org/10.1038/355564a0
92. Tang Z, Parekh P, Turner P, Moyer RW, Tan W (2009) Generating aptamers for recognition of virus-infected cells. Clin Chem 55(4):813–822. https://doi.org/10.1373/clinchem.2008.113514
93. Bruno JG, Kiel JL (1999) In vitro selection of DNA aptamers to anthrax spores with electrochemiluminescence detection. Biosens Bioelectron 14(5):457–464. https://doi.org/10.1016/s0956-5663(99)00028-7
94. Shangguan D, Li Y, Tang Z, Cao ZC, Chen HW, Mallikaratchy P, Sefah K, Yang CJ, Tan W (2006) Aptamers evolved from live cells as effective molecular probes for cancer study. Proc Natl Acad Sci U S A 103(32):11838–11843. https://doi.org/10.1073/pnas.0602615103
95. Tang Z, Shangguan D, Wang K, Shi H, Sefah K, Mallikratchy P, Chen HW, Li Y, Tan W (2007) Selection of aptamers for molecular recognition and characterization of cancer cells. Anal Chem 79(13):4900–4907. https://doi.org/10.1021/ac070189y
96. Kopra K, Syrjänpää M, Hänninen P, Härmä H (2014) Non-competitive aptamer-based quenching resonance energy transfer assay for homogeneous growth factor quantification. Analyst 139(8):2016–2023. https://doi.org/10.1039/C3AN01814H
97. Cho H, Yeh E-C, Sinha R, Laurence TA, Bearinger JP, Lee LP (2012) Single-step nanoplasmonic VEGF165 aptasensor for early cancer diagnosis. ACS Nano 6(9):7607–7614. https://doi.org/10.1021/nn203833d
98. Hori S-I, Herrera A, Rossi JJ, Zhou J (2018) Current advances in aptamers for cancer diagnosis and therapy. Cancers 10(1):9. https://doi.org/10.3390/cancers10010009
99. Yousefi M, Dehghani S, Nosrati R, Zare H, Evazalipour M, Mosafer J, Tehrani BS, Pasdar A, Mokhtarzadeh A, Ramezani M (2019) Aptasensors as a new sensing technology developed for the detection of MUC1 mucin: a review. Biosens Bioelectron 130:1–19. https://doi.org/10.1016/j.bios.2019.01.015
100. Dehghani S, Nosrati R, Yousefi M, Nezami A, Soltani F, Taghdisi SM, Abnous K, Alibolandi M, Ramezani M (2018) Aptamer-based biosensors and nanosensors for the detection of vascular endothelial growth factor (VEGF): a review. Biosens Bioelectron 110:23–37. https://doi.org/10.1016/j.bios.2018.03.037
101. Chen C, Zhou S, Cai Y, Tang F (2017) Nucleic acid aptamer application in diagnosis and therapy of colorectal cancer based on cell-SELEX technology. npj Precision Oncology 1(1):37. https://doi.org/10.1038/s41698-017-0041-y
102. Cui F, Zhou Z, Zhou HS (2020) Review—measurement and analysis of cancer biomarkers based on electrochemical biosensors. J Electrochem Soc 167(3):037525. https://doi.org/10.1149/2.0252003jes
103. Campuzano S, Pedrero M, Pingarrón MJ (2017) Non-invasive breast cancer diagnosis through electrochemical biosensing at different molecular levels. Sensors 17(9). https://doi.org/10.3390/s17091993
104. Kaur H, Shorie M (2019) Nanomaterial based aptasensors for clinical and environmental diagnostic applications. Nanoscale Advances 1(6):2123–2138. https://doi.org/10.1039/C9NA00153K
105. Li Z, Mohamed MA, Vinu Mohan AM, Zhu Z, Sharma V, Mishra GK, Mishra RK (2019) Application of electrochemical aptasensors toward clinical diagnostics, food, and environmental monitoring: review. Sensors 19(24):5435
106. Díaz-Fernández A, Lorenzo-Gómez R, Miranda-Castro R, de los Santos-Álvarez N, Lobo-Castañón MJ (2020) Electrochemical aptasensors for cancer diagnosis in biological fluids–a review. Analytica Chimica Acta
107. Freeman R, Girsh J, Fang-ju Jou A, Ho J-aA, Hug T, Dernedde J, Willner I (2012) Optical aptasensors for the analysis of the vascular endothelial growth factor (VEGF). Anal Chem 84(14):6192–6198. https://doi.org/10.1021/ac3011473

108. Wang S-E, Si S (2013) A fluorescent nanoprobe based on graphene oxide fluorescence resonance energy transfer for the rapid determination of oncoprotein vascular endothelial growth factor (VEGF). Appl Spectrosc 67(11):1270–1274. https://doi.org/10.1366/13-07071
109. Zhang X, Xiao K, Cheng L, Chen H, Liu B, Zhang S, Kong J (2014) Visual and highly sensitive detection of cancer cells by a colorimetric aptasensor based on cell-triggered cyclic enzymatic signal amplification. Anal Chem 86(11):5567–5572. https://doi.org/10.1021/ac501068k
110. Kwon OS, Park SJ, Hong J-Y, Han AR, Lee JS, Lee JS, Oh JH, Jang J (2012) Flexible FET-type VEGF aptasensor based on nitrogen-doped graphene converted from conducting polymer. ACS Nano 6(2):1486–1493. https://doi.org/10.1021/nn204395n
111. Chen X, Zhang Q, Qian C, Hao N, Xu L, Yao C (2015) Electrochemical aptasensor for mucin 1 based on dual signal amplification of poly(o-phenylenediamine) carrier and functionalized carbon nanotubes tracing tag. Biosens Bioelectron 64:485–492. https://doi.org/10.1016/j.bios.2014.09.052
112. Shan S, He Z, Mao S, Jie M, Yi L, Lin J-M (2017) Quantitative determination of VEGF165 in cell culture medium by aptamer sandwich based chemiluminescence assay. Talanta 171:197–203. https://doi.org/10.1016/j.talanta.2017.04.057
113. Nonaka Y, Abe K, Ikebukuro K (2012) Electrochemical detection of vascular endothelial growth factor with aptamer sandwich. Electrochemistry 80(5):363–366. https://doi.org/10.5796/electrochemistry.80.363
114. Song Y, Zhu Z, An Y, Zhang W, Zhang H, Liu D, Yu C, Duan W, Yang CJ (2013) Selection of DNA aptamers against epithelial cell adhesion molecule for cancer cell imaging and circulating tumor cell capture. Anal Chem 85(8):4141–4149. https://doi.org/10.1021/ac400366b
115. Ahirwar R, Nahar S, Aggarwal S, Ramachandran S, Maiti S, Nahar P (2016) In silico selection of an aptamer to estrogen receptor alpha using computational docking employing estrogen response elements as aptamer-alike molecules. Sci Rep 6(1):21285. https://doi.org/10.1038/srep21285
116. Niazi JH, Verma SK, Niazi S, Qureshi A (2015) In vitro HER2 protein-induced affinity dissociation of carbon nanotube-wrapped anti-HER2 aptamers for HER2 protein detection. Analyst 140(1):243–249. https://doi.org/10.1039/C4AN01665C
117. Liu Z, Duan JH, Song YM, Ma J, Wang FD, Lu X, Yang XD (2012) Novel HER2 aptamer selectively delivers cytotoxic drug to HER2-positive breast cancer cells in vitro. J Transl Med 10:148. https://doi.org/10.1186/1479-5876-10-148
118. Kim MY, Jeong S (2011) In vitro selection of RNA aptamer and specific targeting of ErbB2 in breast cancer cells. Nucleic acid therapeutics 21(3):173–178. https://doi.org/10.1089/nat.2011.0283
119. Sett A, Borthakur BB, Bora U (2017) Selection of DNA aptamers for extra cellular domain of human epidermal growth factor receptor 2 to detect HER2 positive carcinomas. Clin Transl Oncol 19(8):976–988. https://doi.org/10.1007/s12094-017-1629-y
120. Cheng AKH, Su H, Wang YA, Yu H-Z (2009) Aptamer-based detection of epithelial tumor marker mucin 1 with quantum dot-based fluorescence readout. Anal Chem 81(15):6130–6139. https://doi.org/10.1021/ac901223q
121. Cao H, Fang X, Li H, Li H, Kong J (2017) Ultrasensitive detection of mucin 1 biomarker by immuno-loop-mediated isothermal amplification. Talanta 164:588–592. https://doi.org/10.1016/j.talanta.2016.07.018
122. Ferreira CSM, Papamichael K, Guilbault G, Schwarzacher T, Gariepy J, Missailidis S (2008) DNA aptamers against the MUC1 tumour marker: design of aptamer–antibody sandwich ELISA for the early diagnosis of epithelial tumours. Anal Bioanal Chem 390(4):1039–1050. https://doi.org/10.1007/s00216-007-1470-1
123. Nonaka Y, Sode K, Ikebukuro K (2010) Screening and improvement of an anti-VEGF DNA aptamer. Molecules 15(1). https://doi.org/10.3390/molecules15010215
124. Potty AS, Kourentzi K, Fang H, Jackson GW, Zhang X, Legge GB, Willson RC (2009) Biophysical characterization of DNA aptamer interactions with vascular endothelial growth factor. Biopolymers 91(2):145–156. https://doi.org/10.1002/bip.21097
125. Kwon OS, Park SJ, Jang J (2010) A high-performance VEGF aptamer functionalized polypyrrole nanotube biosensor. Biomaterials 31(17):4740–4747. https://doi.org/10.1016/j.biomaterials.2010.02.040
126. Chattaraj R, Mohan P, Livingston CM, Besmer JD, Kumar K, Goodwin AP (2016) Mutually-reactive, fluorogenic hydrocyanine/quinone reporter pairs for in-solution biosensing via nanodroplet association. ACS Appl Mater Interfaces 8(1):802–808. https://doi.org/10.1021/acsami.5b10036
127. Sosic A, Meneghello A, Antognoli A, Cretaio E, Gatto B (2013) Development of a multiplex sandwich aptamer microarray for the detection of VEGF165 and thrombin. Sensors 13(10):13425–13438
128. Nonaka Y, Yoshida W, Abe K, Ferri S, Schulze H, Bachmann TT, Ikebukuro K (2013) Affinity improvement of a VEGF aptamer by in silico maturation for a sensitive VEGF-detection system. Anal Chem 85(2):1132–1137. https://doi.org/10.1021/ac303023d
129. Wang S-E, Huang Y, Hu K, Tian J, Zhao S (2014) A highly sensitive and selective aptasensor based on fluorescence polarization for the rapid determination of oncoprotein vascular endothelial growth factor (VEGF). Anal Methods 6(1):62–66. https://doi.org/10.1039/C3AY41697F
130. Lin X, Chen Q, Liu W, Yi L, Li H, Wang Z, Lin J-M (2015) Assay of multiplex proteins from cell metabolism based on tunable aptamer and microchip electrophoresis. Biosens Bioelectron 63:105–111. https://doi.org/10.1016/j.bios.2014.07.013
131. Kaur H, Yung L-YL (2012) Probing high affinity sequences of DNA aptamer against VEGF165. PLoS One 7(2):e31196. https://doi.org/10.1371/journal.pone.0031196
132. Zhang M, Gao G, Ding Y, Deng C, Xiang J, Wu H (2019) A fluorescent aptasensor for the femtomolar detection of epidermal growth factor receptor-2 based on the proximity of G-rich sequences to Ag nanoclusters. Talanta 199:238–243. https://doi.org/10.1016/j.talanta.2019.02.014
133. Xu J, Chen W, Shi M, Huang Y, Fang L, Zhao S, Yao L, Liang H (2019) An aptamer-based four-color fluorometic method for simultaneous determination and imaging of alpha-fetoprotein, vascular endothelial growth factor-165, carcinoembryonic antigen and human epidermal growth factor receptor 2 in living cells. Microchim Acta 186(3). https://doi.org/10.1007/s00604-019-3312-1
134. He Y, Lin Y, Tang H, Pang D (2012) A graphene oxide-based fluorescent aptasensor for the turn-on detection of epithelial tumor marker mucin 1. Nanoscale 4(6):2054–2059. https://doi.org/10.1039/C2NR12061E
135. Ding Y, Ling J, Wang H, Zou J, Wang K, Xiao X, Yang M (2015) Fluorescent detection of Mucin 1 protein based on aptamer functionalized biocompatible carbon dots and graphene oxide. Anal Methods 7(18):7792–7798. https://doi.org/10.1039/c5ay01680k
136. Ma N, Jiang W, Li T, Zhang Z, Qi H, Yang M (2015) Fluorescence aggregation assay for the protein biomarker mucin 1 using carbon dot-labeled antibodies and aptamers. Microchim Acta 182(1–2):443–447. https://doi.org/10.1007/s00604-014-1386-3
137. Li C, Meng Y, Wang S, Qian M, Wang J, Lu W, Huang R (2015) Mesoporous carbon nanospheres featured fluorescent aptasensor

for multiple diagnosis of cancer in vitro and in vivo. ACS Nano 9(12):12096–12103. https://doi.org/10.1021/acsnano.5b05137
138. Zhang Y, Guo S, Huang H, Mao G, Ji X, He Z (2018) Silicon nanodot-based aptasensor for fluorescence turn-on detection of mucin 1 and targeted cancer cell imaging. Anal Chim Acta 1035:154–160. https://doi.org/10.1016/j.aca.2018.06.032
139. Liu H, Zhang L, Xu Y, Chen J, Wang Y, Huang Q, Chen X, Liu Y, Dai Z, Zou X, Li Z (2019) Sandwich immunoassay coupled with isothermal exponential amplification reaction: an ultrasensitive approach for determination of tumor marker MUC1. Talanta 204:248–254. https://doi.org/10.1016/j.talanta.2019.06.001
140. Fan X, Qin Y, Jiang B, Yuan R, Xiang Y (2020) Target-induced autonomous synthesis of G-quadruplex sequences for label-free and amplified fluorescent aptasensing of mucin 1. Sensors and Actuators, B: Chemical 304. doi:https://doi.org/10.1016/j.snb.2019.127351
141. Wang DE, Gao X, You S, Chen M, Ren L, Sun W, Yang H, Xu H (2020) Aptamer-functionalized polydiacetylene liposomes act as a fluorescent sensor for sensitive detection of MUC1 and targeted imaging of cancer cells. Sensors Actuators B Chem 309. https://doi.org/10.1016/j.snb.2020.127778
142. Li J, Liu J, Bi Y, Sun M, Bai J, Zhou M (2020) Ultrasensitive electrochemiluminescence biosensing platform for miRNA-21 and MUC1 detection based on dual catalytic hairpin assembly. Anal Chim Acta 1105:87–94. https://doi.org/10.1016/j.aca.2020.01.034
143. Li W, Zhang Q, Zhou H, Chen J, Li Y, Zhang C, Yu C (2015) Chemiluminescence detection of a protein through the aptamer-controlled catalysis of a porphyrin probe. Anal Chem 87(16):8336–8341. https://doi.org/10.1021/acs.analchem.5b01511
144. Zhang H, Li M, Li C, Guo Z, Dong H, Wu P, Cai C (2015) G-quadruplex DNAzyme-based electrochemiluminescence biosensing strategy for VEGF165 detection: combination of aptamer–target recognition and T7 exonuclease-assisted cycling signal amplification. Biosens Bioelectron 74:98–103. https://doi.org/10.1016/j.bios.2015.05.069
145. Mita C, Abe K, Fukaya T, Ikebukuro K (2014) Vascular endothelial growth factor (VEGF) detection using an aptamer and PNA-based bound/free separation system. Materials 7(2):1046–1054
146. Moghadam FM, Rahaie M (2019) A signal-on nanobiosensor for VEGF 165 detection based on supraparticle copper nanoclusters formed on bivalent aptamer. Biosens Bioelectron 132:186–195. https://doi.org/10.1016/j.bios.2019.02.046
147. Valeur B, Berberan-Santos MN (2011) A brief history of fluorescence and phosphorescence before the emergence of quantum theory. J Chem Educ 88(6):731–738. https://doi.org/10.1021/ed100182h
148. Degliangeli F, Kshirsagar P, Brunetti V, Pompa PP, Fiammengo R (2014) Absolute and direct microRNA quantification using DNA–gold nanoparticle probes. J Am Chem Soc 136(6):2264–2267. https://doi.org/10.1021/ja412152x
149. Shi J, Tian F, Lyu J, Yang M (2015) Nanoparticle based fluorescence resonance energy transfer (FRET) for biosensing applications. J Mater Chem B 3(35):6989–7005. https://doi.org/10.1039/C5TB00885A
150. Murthy KVR, Virk HS (2014) Luminescence phenomena: an introduction. Defect and Diffusion Forum 347:1–34. https://doi.org/10.4028/www.scientific.net/DDF.347.1
151. Ronda C, Srivastava A (2006) Luminescence science and display materials. Electrochemical Society Interface 15(1):55–57
152. Chang C-C, Chen C-Y, Chuang T-L, Wu T-H, Wei S-C, Liao H, Lin C-W (2016) Aptamer-based colorimetric detection of proteins using a branched DNA cascade amplification strategy and unmodified gold nanoparticles. Biosens Bioelectron 78:200–205. https://doi.org/10.1016/j.bios.2015.11.051
153. Wu L, Wang J, Feng L, Ren J, Wei W, Qu X (2012) Label-free ultrasensitive detection of human telomerase activity using porphyrin-functionalized graphene and electrochemiluminescence technique. Adv Mater 24(18):2447–2452. https://doi.org/10.1002/adma.201200412
154. Mansuriya BD, Altintas Z (2020) Applications of graphene quantum dots in biomedical sensors. Sensors (Basel, Switzerland) 20(4):1072. https://doi.org/10.3390/s20041072
155. Banerjee A, Pons T, Lequeux N, Dubertret B (2016) Quantum dots-DNA bioconjugates: synthesis to applications. Interface focus 6(6):20160064–20160064. https://doi.org/10.1098/rsfs.2016.0064
156. Jin S, Hu Y, Gu Z, Liu L, Wu H-C (2011) Application of quantum dots in biological imaging. J Nanomater 2011
157. Song C, Zhang S, Zhou Q, Hai H, Zhao D, Hui Y (2017) Upconversion nanoparticles for bioimaging. Nanotechnol Rev 6(2):233–242. https://doi.org/10.1515/ntrev-2016-0043
158. Wang M, Abbineni G, Clevenger A, Mao C, Xu S (2011) Upconversion nanoparticles: synthesis, surface modification and biological applications. Nanomedicine 7(6):710–729. https://doi.org/10.1016/j.nano.2011.02.013
159. Pan L-H, Kuo S-H, Lin T-Y, Lin C-W, Fang P-Y, Yang H-W (2017) An electrochemical biosensor to simultaneously detect VEGF and PSA for early prostate cancer diagnosis based on graphene oxide/ssDNA/PLLA nanoparticles. Biosens Bioelectron 89:598–605. https://doi.org/10.1016/j.bios.2016.01.077
160. Charbgoo F, Soltani F, Taghdisi SM, Abnous K, Ramezani M (2016) Nanoparticles application in high sensitive aptasensor design. TrAC Trends Anal Chem 85:85–97. https://doi.org/10.1016/j.trac.2016.08.008
161. Wu CH, Huang YY, Chen P, Hoshino K, Liu H, Frenkel EP, Zhang JX, Sokolov KV (2013) Versatile immunomagnetic nanocarrier platform for capturing cancer cells. ACS Nano 7(10):8816–8823. https://doi.org/10.1021/nn403281e
162. Du Y, Dong S (2017) Nucleic acid biosensors: recent advances and perspectives. Anal Chem 89(1):189–215. https://doi.org/10.1021/acs.analchem.6b04190
163. Zhang H, Peng L, Li M, Ma J, Qi S, Chen H, Zhou L, Chen X (2017) A label-free colorimetric biosensor for sensitive detection of vascular endothelial growth factor-165. Analyst 142(13):2419–2425. https://doi.org/10.1039/C7AN00541E
164. Yoo SM, Lee SY (2016) Optical biosensors for the detection of pathogenic microorganisms. Trends Biotechnol 34(1):7–25. https://doi.org/10.1016/j.tibtech.2015.09.012
165. Ranganathan V, Srinivasan S, Singh A, DeRosa MC (2020) An aptamer-based colorimetric lateral flow assay for the detection of human epidermal growth factor receptor 2 (HER2). Anal Biochem 588. https://doi.org/10.1016/j.ab.2019.113471
166. Liu S, Xu N, Tan C, Fang W, Tan Y, Jiang Y (2018) A sensitive colorimetric aptasensor based on trivalent peroxidase-mimic DNAzyme and magnetic nanoparticles. Anal Chim Acta 1018:86–93. https://doi.org/10.1016/j.aca.2018.01.040
167. Zhao S, Ma W, Xu L, Wu X, Kuang H, Wang L, Xu C (2015) Ultrasensitive SERS detection of VEGF based on a self-assembled Ag ornamented–AU pyramid superstructure. Biosens Bioelectron 68:593–597. https://doi.org/10.1016/j.bios.2015.01.056
168. Kim JH, Suh JS, Yang J (2020) Labeling-free detection of ECD-HER2 protein using aptamer-based nano-plasmonic sensor. Nanotechnology 31(17). https://doi.org/10.1088/1361-6528/ab68fa
169. Li Y, Lee HJ, Corn RM (2007) Detection of protein biomarkers using RNA aptamer microarrays and enzymatically amplified surface plasmon resonance imaging. Anal Chem 79(3):1082–1088. https://doi.org/10.1021/ac061849m

170. Chen Y, Nakamoto K, Niwa O, Corn RM (2012) On-chip synthesis of RNA aptamer microarrays for multiplexed protein biosensing with SPR imaging measurements. Langmuir 28(22):8281–8285. https://doi.org/10.1021/la300656c
171. Chen H, Hou Y, Qi F, Zhang J, Koh K, Shen Z, Li G (2014) Detection of vascular endothelial growth factor based on rolling circle amplification as a means of signal enhancement in surface plasmon resonance. Biosens Bioelectron 61:83–87. https://doi.org/10.1016/j.bios.2014.05.005
172. Sigal GB, Mrksich M, Whitesides GM (1997) Using surface plasmon resonance spectroscopy to measure the association of detergents with self-assembled monolayers of hexadecanethiolate on gold. Langmuir 13(10):2749–2755
173. Han X, Liu K, Sun C (2019) Plasmonics for biosensing. Materials (Basel, Switzerland) 12(9):1411. https://doi.org/10.3390/ma12091411
174. Wong CL, Olivo M (2014) Surface plasmon resonance imaging sensors: a review. Plasmonics 9(4):809–824. https://doi.org/10.1007/s11468-013-9662-3
175. Špačková B, Wrobel P, Bocková M, Homola J (2016) Optical biosensors based on plasmonic nanostructures: a review. Proc IEEE 104(12):2380–2408. https://doi.org/10.1109/JPROC.2016.2624340
176. Stiles PL, Dieringer JA, Shah NC, Duyne RPV (2008) Surface-enhanced Raman spectroscopy. Annu Rev Anal Chem 1(1):601–626. https://doi.org/10.1146/annurev.anchem.1.031207.112814
177. Mosier-Boss PA (2017) Review of SERS substrates for chemical sensing. Nanomaterials (Basel, Switzerland) 7(6):142. https://doi.org/10.3390/nano7060142
178. Laing S, Jamieson LE, Faulds K, Graham D (2017) Surface-enhanced Raman spectroscopy for in vivo biosensing. Nature Reviews Chemistry 1(8):0060. https://doi.org/10.1038/s41570-017-0060
179. Hodnik V, Anderluh G (2009) Toxin detection by surface plasmon resonance. Sensors (Basel, Switzerland) 9(3):1339–1354. https://doi.org/10.3390/s9031339
180. Poltronieri P, Mezzolla V, Primiceri E, Maruccio G (2014) Biosensors for the detection of food pathogens. Foods (Basel, Switzerland) 3(3):511–526. https://doi.org/10.3390/foods3030511
181. Sahoo PR, Swain P, Nayak SM, Bag S, Mishra SR (2016) Surface plasmon resonance based biosensor: a new platform for rapid diagnosis of livestock diseases. Veterinary world 9(12):1338–1342. https://doi.org/10.14202/vetworld.2016.1338-1342
182. Minunni M, Bilia AR (2009) SPR in drug discovery: searching bioactive compounds in plant extracts. Methods Mol Biol 572:203–218. https://doi.org/10.1007/978-1-60761-244-5_13
183. Masson J-F (2017) Surface plasmon resonance clinical biosensors for medical diagnostics. ACS Sensors 2(1):16–30. https://doi.org/10.1021/acssensors.6b00763
184. Zhu C, Yang G, Li H, Du D, Lin Y (2015) Electrochemical sensors and biosensors based on nanomaterials and nanostructures. Anal Chem 87(1):230–249. https://doi.org/10.1021/ac5039863
185. Luo X, Davis JJ (2013) Electrical biosensors and the label free detection of protein disease biomarkers. Chem Soc Rev 42(13):5944–5962. https://doi.org/10.1039/c3cs60077g
186. Hammond Jules L, Formisano N, Estrela P, Carrara S, Tkac J (2016) Electrochemical biosensors and nanobiosensors. Essays Biochem 60(1):69–80. https://doi.org/10.1042/ebc20150008
187. Ou D, Sun D, Lin X, Liang Z, Zhong Y, Chen Z (2019) A dual-aptamer-based biosensor for specific detection of breast cancer biomarker HER2 via flower-like nanozymes and DNA nanostructures. J Mater Chem B 7(23):3661–3669. https://doi.org/10.1039/c9tb00472f
188. Rostamabadi PF, Heydari-Bafrooei E (2019) Impedimetric aptasensing of the breast cancer biomarker HER2 using a glassy carbon electrode modified with gold nanoparticles in a composite consisting of electrochemically reduced graphene oxide and single-walled carbon nanotubes. Microchim Acta 186(8). https://doi.org/10.1007/s00604-019-3619-y
189. Qureshi A, Gurbuz Y, Niazi JH (2015) Label-free capacitance based aptasensor platform for the detection of HER2/ErbB2 cancer biomarker in serum. Sensors Actuators B Chem 220:1145–1151. https://doi.org/10.1016/j.snb.2015.06.094
190. Arya SK, Zhurauski P, Jolly P, Batistuti MR, Mulato M, Estrela P (2018) Capacitive aptasensor based on interdigitated electrode for breast cancer detection in undiluted human serum. Biosens Bioelectron 102:106–112. https://doi.org/10.1016/j.bios.2017.11.013
191. Zhou N, Su F, Li Z, Yan X, Zhang C, Hu B, He L, Wang M, Zhang Z (2019) Gold nanoparticles conjugated to bimetallic manganese(II) and iron(II) Prussian Blue analogues for aptamer-based impedimetric determination of the human epidermal growth factor receptor-2 and living MCF-7 cells. Microchim Acta 186(2):75. https://doi.org/10.1007/s00604-018-3184-9
192. Qureshi A, Gurbuz Y, Niazi JH (2015) Capacitive aptamer–antibody based sandwich assay for the detection of VEGF cancer biomarker in serum. Sensors Actuators B Chem 209:645–651. https://doi.org/10.1016/j.snb.2014.12.040
193. Malecka K, Pankratov D, Ferapontova EE (2019) Femtomolar electroanalysis of a breast cancer biomarker HER-2/neu protein in human serum by the cellulase-linked sandwich assay on magnetic beads. Anal Chim Acta 1077:140–149. https://doi.org/10.1016/j.aca.2019.05.052
194. Chen D, Wang D, Hu X, Long G, Zhang Y, Zhou L (2019) A DNA nanostructured biosensor for electrochemical analysis of HER2 using bioconjugate of GNR@Pd SSs—Apt—HRP. Sensors Actuators B Chem 296. https://doi.org/10.1016/j.snb.2019.126650
195. Shen C, Zeng K, Luo J, Li X, Yang M, Rasooly A (2017) Self-assembled DNA generated electric current biosensor for HER2 analysis. Anal Chem 89(19):10264–10269. https://doi.org/10.1021/acs.analchem.7b01747
196. Jarczewska M, Wieczorek J, Malinowska E (2020) Electrochemical Studies on the Binding of Antibody—Aptamer Hybrid Receptor Layers to HAB-one of the possibilities of early detection of cancer disease is the analysis of the presence of protein biomarkers. Herein, we present the studies on the hybrid antibody—aptamer receptor layers for electrochemical detection of HER2 protein that is known as a biomarker of e.g. breast cancer. The application of MB-labelled aptamer did not allow to evidence the interaction with HER2 protein. Moreover, the use of unlabelled aptamer as a capture element and polyclonal antibody as a reporter probe did not show a dependence of current signal change vs HER2 protein concentration as well. On the contrary, the application of monoclonal antibody as a capture probe and aptamer labelled at 3′ end with MB as reporter probe enabled the determination of HER2 within 0.01–10 ng·ml−1 concentration range. The elaborated affinity assay also showed good selectivity towards HER2 biomarker and was used for HER2 determination in spiked serum sample. ER2 Protein. Journal of The Electrochemical Society 167(6):067512. https://doi.org/10.1149/1945-7111/ab80ac
197. Tabasi A, Noorbakhsh A, Sharifi E (2017) Reduced graphene oxide-chitosan-aptamer interface as new platform for ultrasensitive detection of human epidermal growth factor receptor 2. Biosens Bioelectron 95:117–123. https://doi.org/10.1016/j.bios.2017.04.020
198. Huang J, Luo X, Lee I, Hu Y, Cui XT, Yun M (2011) Rapid real-time electrical detection of proteins using single conducting polymer nanowire-based microfluidic aptasensor. Biosens Bioelectron 30(1):306–309. https://doi.org/10.1016/j.bios.2011.08.016

199. Florea A, Ravalli A, Cristea C, Săndulescu R, Marrazza G (2015) An optimized bioassay for Mucin1 detection in serum samples. Electroanalysis 27(7):1594–1601. https://doi.org/10.1002/elan.201400689
200. Liu C, Liu X, Qin Y, Deng C, Xiang J (2016) A simple regenerable electrochemical aptasensor for the parallel and continuous detection of biomarkers. RSC Adv 6(63):58469–58476. https://doi.org/10.1039/C6RA09284E
201. Deng C, Pi X, Qian P, Chen X, Wu W, Xiang J (2017) High-performance ratiometric electrochemical method based on the combination of signal probe and inner reference probe in one hairpin-structured DNA. Anal Chem 89(1):966–973. https://doi.org/10.1021/acs.analchem.6b04209
202. Karpik AE, Crulhas BP, Rodrigues CB, Castro GR, Pedrosa VA (2017) Aptamer-based biosensor developed to monitor MUC1 released by prostate cancer cells. Electroanalysis 29(10):2246–2253. https://doi.org/10.1002/elan.201700318
203. Gupta P, Bharti A, Kaur N, Singh S, Prabhakar N (2018) An electrochemical aptasensor based on gold nanoparticles and graphene oxide doped poly(3,4-ethylenedioxythiophene) nanocomposite for detection of MUC1. Journal of Electroanalytical Chemistry 813:102–108. https://doi.org/10.1016/j.jelechem.2018.02.014
204. Yang S, Zhang F, Liang Q, Wang Z (2018) A three-dimensional graphene-based ratiometric signal amplification aptasensor for MUC1 detection. Biosens Bioelectron 120:85–92. https://doi.org/10.1016/j.bios.2018.08.036
205. Wang H, Sun J, Lu L, Yang X, Xia J, Zhang F, Wang Z (2020) Competitive electrochemical aptasensor based on a cDNA-ferrocene/MXene probe for detection of breast cancer marker Mucin1. Anal Chim Acta 1094:18–25. https://doi.org/10.1016/j.aca.2019.10.003
206. Ravalli A, Rivas L, De la Escosura-Muniz A, Pons J, Merkoci A, Marrazza G (2015) A DNA aptasensor for electrochemical detection of vascular endothelial growth factor. J Nanosci Nanotechnol 15 (5):3411–3416. doi:https://doi.org/10.1166/jnn.2015.10037
207. Lv Z, Wang K, Zhang X (2014) A new electrochemical aptasensor for the analysis of the vascular endothelial growth factor. J Immunoass Immunochem 35(3):233–240. https://doi.org/10.1080/15321819.2013.841194
208. Crulhas BP, Karpik AE, Delella FK, Castro GR, Pedrosa VA (2017) Electrochemical aptamer-based biosensor developed to monitor PSA and VEGF released by prostate cancer cells. Anal Bioanal Chem 409(29):6771–6780. https://doi.org/10.1007/s00216-017-0630-1
209. Cheng W, Ding S, Li Q, Yu T, Yin Y, Ju H, Ren G (2012) A simple electrochemical aptasensor for ultrasensitive protein detection using cyclic target-induced primer extension. Biosens Bioelectron 36(1):12–17. https://doi.org/10.1016/j.bios.2012.03.032
210. Da H, Liu H, Zheng Y, Yuan R, Chai Y (2018) A highly sensitive VEGF165 photoelectrochemical biosensor fabricated by assembly of aptamer bridged DNA networks. Biosens Bioelectron 101:213–218. https://doi.org/10.1016/j.bios.2017.10.032
211. Abe K, Hasegawa H, Ikebukuro K (2012) Electrochemical detection of vascular endothelial growth factor by an aptamer-based bound/free separation system. Electrochemistry 80(5):348–352. https://doi.org/10.5796/electrochemistry.80.348
212. Feng L, Lyu Z, Offenhäusser A, Mayer D (2016) Electrochemically triggered aptamer immobilization via click reaction for vascular endothelial growth factor detection. Engineering in Life Sciences 16(6):550–559. https://doi.org/10.1002/elsc.201600068
213. Shamsipur M, Farzin L, Amouzadeh Tabrizi M, Molaabasi F (2015) Highly sensitive label free electrochemical detection of VGEF165 tumor marker based on "signal off" and "signal on" strategies using an anti-VEGF165 aptamer immobilized BSA-gold nanoclusters/ionic liquid/glassy carbon electrode. Biosens Bioelectron 74:369–375. https://doi.org/10.1016/j.bios.2015.06.079
214. Amouzadeh Tabrizi M, Shamsipur M, Saber R, Sarkar S (2017) Simultaneous determination of CYC and VEGF165 tumor markers based on immobilization of flavin adenine dinucleotide and thionine as probes on reduced graphene oxide-poly(amidoamine)/gold nanocomposite modified dual working screen-printed electrode. Sensors Actuators B Chem 240:1174–1181. https://doi.org/10.1016/j.snb.2016.09.108
215. Lee H-S, Kim KS, Kim C-J, Hahn SK, Jo M-H (2009) Electrical detection of VEGFs for cancer diagnoses using anti-vascular endotherial growth factor aptamer-modified Si nanowire FETs. Biosens Bioelectron 24(6):1801–1805. https://doi.org/10.1016/j.bios.2008.08.036
216. Wang B, Akiba U, Anzai J-i (2017) Recent progress in nanomaterial-based electrochemical biosensors for cancer biomarkers: a review. Molecules 22(7):1048
217. Byon HR, Choi HC (2006) Network single-walled carbon nanotube-field effect transistors (SWNT-FETs) with increased Schottky contact area for highly sensitive biosensor applications. J Am Chem Soc 128(7):2188–2189. https://doi.org/10.1021/ja056897n
218. Vu C-A, Chen W-Y (2019) Field-effect transistor biosensors for biomedical applications: recent advances and future prospects. Sensors (Basel, Switzerland) 19(19):4214. https://doi.org/10.3390/s19194214
219. Vu C-A, Chen W-Y (2020) Predicting future prospects of aptamers in field-effect transistor biosensors. Molecules 25(3):680
220. Chen A, Yang S (2015) Replacing antibodies with aptamers in lateral flow immunoassay. Biosens Bioelectron 71:230–242
221. Zhou W, Xu F, Li D, Chen Y (2018) Improved detection of HER2 by a quasi-targeted proteomics approach using aptamer-peptide probe and liquid chromatography-tandem mass spectrometry. Clin Chem 64(3):526–535. https://doi.org/10.1373/clinchem.2017.274266
222. Mei Y-B, Luo S-B, Ye L-Y, Zhang Q, Guo J, Qiu X-J, Xie S-L (2019) Validated UPLC-MS/MS method for quantification of fruquintinib in rat plasma and its application to pharmacokinetic study. Drug design, development and therapy 13:2865–2871. https://doi.org/10.2147/DDDT.S199362
223. Li C, Zhang M, Zhang Z, Tang J, Zhang B (2019) Microcantilever aptasensor for detecting epithelial tumor marker Mucin 1 and diagnosing human breast carcinoma MCF-7 cells. Sensors Actuators B Chem 297. https://doi.org/10.1016/j.snb.2019.126759
224. Shamsipur M, Emami M, Farzin L, Saber R (2018) A sandwich-type electrochemical immunosensor based on in situ silver deposition for determination of serum level of HER2 in breast cancer patients. Biosens Bioelectron 103:54–61. https://doi.org/10.1016/j.bios.2017.12.022
225. Li S, Zheng Y, Liu Y, Geng X, Liu X, Zou L, Wang Q, Yang X, Wang K (2020) Investigation of the interaction between split aptamer and vascular endothelial growth factor 165 using single molecule force spectroscopy. J Mol Recognit 33(5). https://doi.org/10.1002/jmr.2829
226. Johari-Ahar M, Karami P, Ghanei M, Afkhami A, Bagheri H (2018) Development of a molecularly imprinted polymer tailored on disposable screen-printed electrodes for dual detection of EGFR and VEGF using nano-liposomal amplification strategy. Biosens Bioelectron 107:26–33. https://doi.org/10.1016/j.bios.2018.02.005
227. Pacheco JG, Rebelo P, Freitas M, Nouws HPA, Delerue-Matos C (2018) Breast cancer biomarker (HER2-ECD) detection using a molecularly imprinted electrochemical sensor. Sensors Actuators

B Chem 273:1008–1014. https://doi.org/10.1016/j.snb.2018.06.113

228. Pei X, Zhang J, Liu J (2014) Clinical applications of nucleic acid aptamers in cancer. Mol Clin Oncol 2(3):341–348. https://doi.org/10.3892/mco.2014.255
229. Palmirotta R, Lovero D, Cafforio P, Felici C, Mannavola F, Pellè E, Quaresmini D, Tucci M, Silvestris F (2018) Liquid biopsy of cancer: a multimodal diagnostic tool in clinical oncology. Therapeutic advances in medical oncology 10: 1758835918794630–1758835918794630. https://doi.org/10.1177/1758835918794630
230. Agrawal L, Engel KB, Greytak SR, Moore HM (2018) Understanding preanalytical variables and their effects on clinical biomarkers of oncology and immunotherapy. Semin Cancer Biol 52(Pt 2):26–38. https://doi.org/10.1016/j.semcancer.2017.12.008
231. Venook AP, Arcila ME, Benson AB 3rd, Berry DA, Camidge DR, Carlson RW, Choueiri TK, Guild V, Kalemkerian GP, Kurzrock R, Lovly CM, McKee AE, Morgan RJ, Olszanski AJ, Redman MW, Stearns V, McClure J, Birkeland ML (2014) NCCN Working Group report: designing clinical trials in the era of multiple biomarkers and targeted therapies. Journal of the National Comprehensive Cancer Network : JNCCN 12(11):1629–1649. https://doi.org/10.6004/jnccn.2014.0161
232. Mazaafrianto DN, Maeki M, Ishida A, Tani H, Tokeshi M (2018) Recent microdevice-based aptamer sensors. Micromachines 9(5): 202. https://doi.org/10.3390/mi9050202